

# Tensor-scalar gravity and binary-pulsar experiments

Thibault Damour\*

*Institut des Hautes Etudes Scientifiques, F 91440 Bures-sur-Yvette, France,  
and School of Natural Sciences, Institute for Advanced Study, Olden Lane, Princeton, New Jersey 08540*

Gilles Esposito-Farèse†

*Department of Physics, Brandeis University, Waltham, Massachusetts 02254*

(Received 28 February 1996)

Some recently discovered nonperturbative strong-field effects in tensor-scalar theories of gravitation are interpreted as a scalar analogue of ferromagnetism: “spontaneous scalarization.” This phenomenon leads to very significant deviations from general relativity in conditions involving strong gravitational fields, notably binary-pulsar experiments. Contrary to solar-system experiments, these deviations do not necessarily vanish when the weak-field scalar coupling tends to zero. We compute the scalar “form factors” measuring these deviations, and notably a parameter entering the pulsar timing observable  $\gamma$  through scalar-field-induced variations of the inertia moment of the pulsar. An exploratory investigation of the confrontation between tensor-scalar theories and binary-pulsar experiments shows that nonperturbative scalar field effects are already very tightly constrained by published data on three binary-pulsar systems. We contrast the probing power of pulsar experiments with that of solar-system ones by plotting the regions they exclude in a generic two-dimensional plane of tensor-scalar theories. [S0556-2821(96)04314-7]

PACS number(s): 04.50.+h, 04.80.Cc, 97.60.Gb

## I. INTRODUCTION

Einstein’s general relativity theory postulates that gravity is mediated only by a long-range tensor field. It has been repeatedly pointed out over the years (starting with Kaluza [1]) that unified theories naturally give rise to long-range scalar fields coupled to matter with gravitational strength. This led many authors, notably Jordan [2], Fierz [3], and Brans and Dicke [4], to study, as most natural alternatives to general relativity, tensor-scalar theories in which gravity is mediated in part by a long-range scalar field. The motivation for such theories has been recently revived by string theory which contains massless scalars in its gravitational sector (notably the model-independent dilaton).

We shall consider tensor-scalar gravitation theories containing only one scalar field, assumed to couple to the trace of the energy-momentum tensor. The simplest example of such a theory is a scalar field only coupled to the gravitational sector through a nonminimal coupling  $\xi R\Phi^2$  (see Sec. VI below). For a study of the observable consequences of general tensor-scalar theories (containing one or several scalar fields), see Ref. [5].

Actually, one generically expects scalar fields not to couple exactly to the mass but to exhibit some “composition dependence” in their couplings to matter. However, a recent study of a large class of viable string-inspired tensor-scalar models [6] has found that the composition-dependent effects represent only a very small fraction ( $\sim 10^{-5}$ ) of the effective

coupling to matter. Such fractionally small composition-dependent effects would be negligible in the gravitational physics of neutron stars that we consider here.

The most general theory describing a mass-coupled long-range scalar contains one arbitrary “coupling function”  $A(\varphi)$  [3]. The action defining the theory reads

$$S = \frac{c^4}{16\pi G_*} \int \frac{d^4x}{c} g_*^{1/2} (R_* - 2g_*^{\mu\nu} \partial_\mu \varphi \partial_\nu \varphi) + S_m[\psi_m; A^2(\varphi)g_{\mu\nu}^*]. \quad (1.1)$$

Here,  $G_*$  denotes a bare gravitational coupling constant,  $R_* \equiv g_*^{\mu\nu} R_{\mu\nu}^*$  the curvature scalar of the “Einstein metric”  $g_{\mu\nu}^*$  describing the pure spin-2 excitations, and  $\varphi$  our long-range scalar field describing spin-0 excitations. [We use the signature  $-+++$  and the notation  $g_* \equiv -\det g_{\mu\nu}^*$ .] The last term in Eq. (1.1) denotes the action of matter, which is a functional of some matter variables (collectively denoted by  $\psi_m$ ) and of the “physical metric”  $\tilde{g}_{\mu\nu} \equiv A^2(\varphi)g_{\mu\nu}^*$ . Laboratory clocks and rods measure the metric  $\tilde{g}_{\mu\nu}$  which, in the model considered here, is universally coupled to matter. The reader will find in Eqs. (6.1)–(6.7) below an explicit example (nonminimally coupled scalar field) of how an action of the type (1.1), involving two conformally related metrics  $g_{\mu\nu}^*$  and  $\tilde{g}_{\mu\nu} = A^2(\varphi)g_{\mu\nu}^*$ , can naturally arise.

The field equations of the theory are most simply formulated in terms of the pure-spin variables  $(g_{\mu\nu}^*, \varphi)$ . Varying the action (1.1) yields

$$R_{\mu\nu}^* = 2\partial_\mu \varphi \partial_\nu \varphi + \frac{8\pi G_*}{c^4} \left( T_{\mu\nu}^* - \frac{1}{2} T^* g_{\mu\nu}^* \right), \quad (1.2a)$$

\* Also at the Département d’Astrophysique Relativiste et de Cosmologie, Observatoire de Paris, Centre National de la Recherche Scientifique, F 92195 Meudon, France.

† Permanent address: Centre de Physique Théorique, CNRS Luminy, Case 907, F 13288 Marseille Cedex 9, France.

$$\square_{g*}\varphi = -\frac{4\pi G_*}{c^4}\alpha(\varphi)T_*, \quad (1.2b)$$

with  $T_*^{\mu\nu} \equiv 2c g_*^{-1/2} \delta S_m / \delta g_{\mu\nu}^*$  denoting the material stress-energy tensor in ‘‘Einstein units’’ and  $\alpha(\varphi)$  the logarithmic derivative of  $A(\varphi)$ :

$$\alpha(\varphi) \equiv \frac{\partial \ln A(\varphi)}{\partial \varphi}. \quad (1.3)$$

[All tensorial operations in Eqs. (1.2) are performed by using the Einstein metric  $g_{\mu\nu}^*$ , e.g.,  $\square_{g*} \equiv g_{\mu\nu}^* \nabla_\mu^* \nabla_\nu^*$ ,  $T_* \equiv g_{\mu\nu}^* T_*^{\mu\nu}$ .] As is clear from Eq. (1.2b), the quantity  $\alpha(\varphi)$  plays the role of measuring the (field-dependent) *coupling strength* between the scalar field and matter. It has been shown in Refs. [5,7] that all *weak-field* (‘‘post-Newtonian’’) deviations from general relativity (of any post-Newtonian order) can be expressed in terms of the asymptotic value of  $\alpha(\varphi)$  at spatial infinity and of its successive scalar-field derivatives. Let  $\varphi_0$  denote the asymptotic value of  $\varphi$  at spatial infinity, i.e., the ‘‘vacuum expectation value’’ of  $\varphi$  far away from the considered gravitating system. Let us also denote  $\alpha_0 \equiv \alpha(\varphi_0)$ ,  $\beta_0 \equiv \partial \alpha(\varphi_0) / \partial \varphi_0$ , and  $\beta'_0 \equiv \partial \beta(\varphi_0) / \partial \varphi_0$ . At the first post-Newtonian approximation, deviations from general relativity are proportional to the Eddington parameters

$$\bar{\gamma} \equiv \gamma_{\text{Edd}} - 1 = -2\alpha_0^2 / (1 + \alpha_0^2), \quad (1.4a)$$

$$\bar{\beta} \equiv \beta_{\text{Edd}} - 1 = \frac{1}{2}\beta_0\alpha_0^2 / (1 + \alpha_0^2)^2, \quad (1.4b)$$

while at the second post-Newtonian approximation there enters, beyond  $\bar{\gamma}$  and  $\bar{\beta}$ , two new parameters [5,7]

$$\varepsilon = \beta'_0\alpha_0^3 / (1 + \alpha_0^2)^3, \quad (1.5a)$$

$$\zeta = \beta_0^2\alpha_0^2 / (1 + \alpha_0^2)^3. \quad (1.5b)$$

We see explicitly in Eqs. (1.4) and (1.5) that all deviations from general relativity tend to zero with  $\alpha_0$  at least as fast as  $\alpha_0^2$ . This holds true for *weak-field* deviations of arbitrary post-Newtonian order [7]. Therefore, light-deflection or time-delay experiments [8] which set [through Eq. (1.4a)] the following limit on the coupling strength of the scalar field,

$$\alpha_0^2 < 10^{-3}, \quad (1.6)$$

tightly constrain the theoretically expectable<sup>1</sup> level of deviation from general relativity in all other experiments probing weak gravitational fields. Note that, in many physically motivated models, there are much tighter limits on  $\alpha_0^2$  coming from equivalence principle tests (see, e.g., [9], which gets  $\alpha_0^2 \lesssim 10^{-7}$  in string-derived models). These improved limits crucially depend, however, on the detailed structure and magnitude of equivalence-principle-violating effects (and

disappear in the subclass of metrically coupled theories). To stay model independent, we shall use the post-Newtonian-derived limit (1.6) as our standard weak-field limit. As we shall see later, the importance of the nonperturbative effects discussed here is not uniformly decreased when  $\alpha_0$  takes smaller values, but can level off or even be amplified.

In a previous work [10], we have shown that experiments involving the *strong gravitational fields* of neutron stars can exhibit a remarkably different behavior from weak-field solar-system experiments. We proved that when a certain mild inequality restricting the curvature of the coupling function  $\ln A(\varphi)$  was satisfied, namely,

$$\beta_0 \equiv \frac{\partial^2 \ln A(\varphi_0)}{\partial \varphi_0^2} \lesssim -4, \quad (1.7)$$

nonperturbative strong-gravitational-field effects developed in neutron stars and induced order-of-unity deviations from general relativity, even for arbitrary small values of the linear coupling strength  $\alpha_0^2$ . The aim of the present paper is to further study these nonperturbative phenomena and to prepare the ground for a systematic application to binary-pulsar experiments [11] by computing the observational effects depending upon the inertia moments of neutron stars. One of the main results of the present study will be to show explicitly that binary-pulsar experiments are, in some regions of theory space, much more constraining than solar-system experiments. This will be illustrated in an exclusion plot discussed below.

The organization of this paper is as follows. In Sec. II, we show how the nonperturbative scalar-field effects discovered in [10] can be interpreted as a ‘‘spontaneous scalarization’’ of neutron stars, analogous to the spontaneous magnetization of ferromagnets. We write in Sec. III the field equations that must be numerically integrated to study these nonperturbative effects in slowly rotating neutron stars. Section IV discusses the ‘‘gravitational form factors’’ governing the physics of neutron stars in tensor-scalar gravity, notably a parameter linked to the variation of a pulsar’s inertia moment caused by the presence of an orbiting companion. The constraints imposed by three binary-pulsar experiments on a generic class of tensor-scalar models are then derived in Sec. V. Finally, the conclusions of our study are given in Sec. VI.

## II. SPONTANEOUS SCALARIZATION

Before tackling the technical problems posed by the computation of various gravitational ‘‘form factors’’ in presence of strong-scalar-field effects, let us clarify, at the conceptual level, the physical origin of the nonperturbative effect discovered in [10].

Let us consider a very simple coupling function of the form

$$A(\varphi) = A_\beta(\varphi) \equiv \exp\left(\frac{1}{2}\beta\varphi^2\right), \quad (2.1)$$

corresponding to a coupling strength  $\alpha(\varphi) = \partial \ln A(\varphi) / \partial \varphi = \beta\varphi$ , where  $\beta$  is a given parameter. The model (2.1), where  $\ln A(\varphi)$  is quadratic in  $\varphi$ , is second in simplicity to the Jordan-Fierz-Brans-Dicke model where  $\ln A(\varphi) = \alpha_0\varphi$  is lin-

<sup>1</sup>We assume here the absence of unnaturally large dimensionless numbers appearing in the successive derivatives of  $\alpha(\varphi)$ :  $\beta_0$ ,  $\beta'_0$ , . . .

ear in  $\varphi$ . [We shall sometimes refer to model (2.1) as “the quadratic model.”] When  $\beta$  satisfies  $\beta \leq -4$ , we are in a regime where nonperturbative effects develop for massive enough neutron stars. The results of [10] raise a paradox in the limit where the asymptotic value of  $\varphi_0$  tends toward zero, i.e.,  $\alpha_0 = \beta \varphi_0 \rightarrow 0$ . Indeed, in the case  $\alpha = \beta \varphi$  the right-hand side of Eq. (1.2b) is proportional to  $\varphi$ , and  $\varphi(x) \equiv 0$  is an exact solution which satisfies the homogeneous boundary conditions  $\varphi \rightarrow 0$  at spatial infinity. Equation (1.2b) being elliptic in the stationary case of an isolated star, it would seem that the solution, with given boundary conditions, must be unique, and therefore that in the homogeneous case  $\varphi_0 = 0$  the only solution must be the trivial one  $\varphi(x) = 0$ . This conclusion is correct in the case of weakly self-gravitating systems (such as ordinary stars, white dwarfs, or even low-mass neutron stars). Should not then physical continuity require to take always as “correct” solution of Eq. (1.2b) the trivial one, even when considering strongly self-gravitating systems such as neutron stars? What can cause a discontinuity in the configuration of the scalar field (with homogeneous boundary condition) for massive neutron stars? In the simple case of the coupling function (2.1), we have the further paradox that the theory is symmetric under the reflection  $\varphi \rightarrow -\varphi$ , so that it seems at face value that the solution of Eqs. (1.2) corresponding to the self-symmetric boundary conditions  $\varphi_0 = 0$  must be self-symmetric and therefore identically zero.

A solution of these paradoxes, and a clearer understanding of the phenomena studied in [10], is obtained by making an analogy with the well-known phenomenon of spontaneous magnetization of ferromagnets (below the Curie temperature). In the latter case, a convenient order parameter is the total magnetization  $\mathbf{M}$  (which is thermodynamically conjugate to the external magnetic field  $\mathbf{B}_0$ :  $\mathbf{M} = -\partial E / \partial \mathbf{B}_0$ ). In our “scalarization” case, we can take as order parameter the total scalar charge  $\omega_A$  developed by the neutron star (labeled A) in presence of an external scalar field  $\varphi_0$ ; it is defined as the coefficient of  $G_*/r$  in the far scalar field around A:  $\varphi(r) = \varphi_0 + G_* \omega_A / r + O(1/r^2)$  as  $r \rightarrow \infty$ . As shown in [5],  $\omega_A$  is energetically conjugate to the external scalar field  $\varphi_0$ :

$$\omega_A = -\partial m_A / \partial \varphi_0, \quad (2.2)$$

where  $m_A$  denotes the total mass-energy of the star (in Einstein units). It is also the quantity which appears directly in the Keplerian-order interaction energy between two stars:  $V_{\text{int}} = -G_* m_A m_B / r_{AB} - G_* \omega_A \omega_B / r_{AB}$ , where the first term comes from the exchange of a graviton and the second from the exchange of a scalaron. In the presence of a nonzero external  $\varphi_0$ , weakly self-gravitating objects develop a scalar charge which is proportional to  $\varphi_0$  in the limit  $\varphi_0 \rightarrow 0$  (“scalar susceptibility,” the analogue to the magnetic susceptibility  $\mathbf{M} = \chi \mathbf{B}_0$  for weak external magnetic fields in the absence of spontaneous magnetization).

Following Landau, we can understand what happens for strongly self-gravitating objects by writing the total energy to be minimized as a function of both the external field and the order parameter,  $m_A(\omega_A, \varphi_0) = \mu(\omega_A) - \omega_A \varphi_0$ , and by assuming that the (Legendre transform) energy function  $\mu(\omega_A)$  develops, when some control parameter varies, a

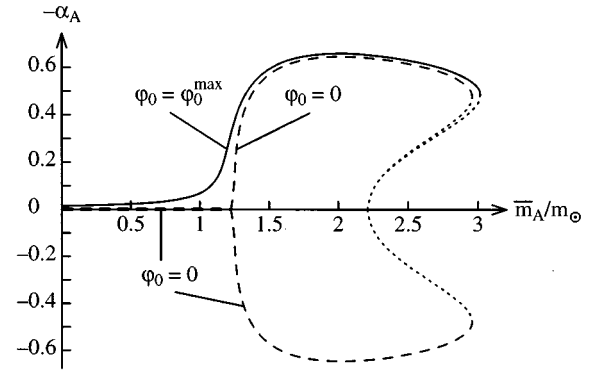


FIG. 1. Effective scalar coupling strength  $-\alpha_A \equiv \omega_A / m_A$  versus baryonic mass  $\bar{m}_A$ , for the model  $A(\varphi) = \exp(-3\varphi^2)$ . The solid line corresponds to the maximum value of  $\varphi_0$  allowed by solar-system experiments, and the dashed lines to  $\varphi_0 = 0$  (“zero mode”). The dotted lines correspond to unstable configurations of the star.

minimum at a nonzero value of  $\omega_A$ . In our case, if we fix the shape of the coupling function  $A(\varphi)$  [for instance Eq. (2.1) with  $\beta$  sufficiently negative], the control parameter is the total baryon mass  $\bar{m}_A$  of the star. A simple model exhibiting the appearance of a “spontaneous scalarization” of a star in absence of external field  $\varphi_0$  is simply the usual Landau ansatz near the critical transition point:  $\mu(\omega_A) = \frac{1}{2}a(\bar{m}_{\text{cr}} - \bar{m}_A)\omega_A^2 + \frac{1}{4}b\omega_A^4$ . In absence of external field,  $\varphi_0 = 0$ , the energy  $m_A$  is minimum at the unique (trivial) solution  $\omega_A = 0$  when  $\bar{m}_A < \bar{m}_{\text{cr}}$ , while when  $\bar{m}_A > \bar{m}_{\text{cr}}$ , there appear two energetically favored nontrivial solutions  $\omega_A = \pm [b^{-1}a(\bar{m}_A - \bar{m}_{\text{cr}})]^{1/2}$ . At the critical transition  $\bar{m}_A = \bar{m}_{\text{cr}}$ , the slope  $d\omega_A/d\bar{m}_A$  is infinite. As in the ferromagnetic case, the presence of an external field  $\varphi_0 \neq 0$  smoothes the transition. For instance, the “scalar susceptibility”  $\chi_A = \partial \omega_A / \partial \varphi_0$  which blows up near the critical point as  $|\bar{m}_A - \bar{m}_{\text{cr}}|^{-1}$  when  $\varphi_0 = 0$  becomes a rapidly varying but smooth function of  $\bar{m}_A$  when  $\varphi_0 \neq 0$ . The results of [10] clearly exhibit the sharpening of the transition as  $\varphi_0 \rightarrow 0$ . This is illustrated in Fig. 1, which displays two curves corresponding to  $\varphi_0 = 2.4 \times 10^{-3}$  and  $\varphi_0 = 0$  for the same theory [ $\beta = -6$  in Eq. (2.1)] and the same equation of state (EOS II of Ref. [12]). Note that, when  $\varphi_0 \neq 0$ , it is the sign of the external  $\varphi_0$  which determines the direction of the symmetry breaking.

It is convenient, notably for the applications to binary-pulsar experiments, to replace the quantity  $\omega_A$  by the related quantity

$$\alpha_A \equiv -\frac{\omega_A}{m_A} \equiv \frac{\partial \ln m_A}{\partial \varphi_0}, \quad (2.3)$$

which measures the effective strength of the coupling between  $\varphi$  and the star. It is the strong-field counterpart of the weak-field coupling strength  $\alpha_0 = \alpha(\varphi_0)$  and reduces to it in the case of negligible self-gravity. Correlatively, it is convenient to replace the scalar susceptibility  $\chi_A = \partial \omega_A / \partial \varphi_0$  by the quantity

$$\beta_A \equiv \frac{\partial \alpha_A}{\partial \varphi_0}, \quad (2.4)$$

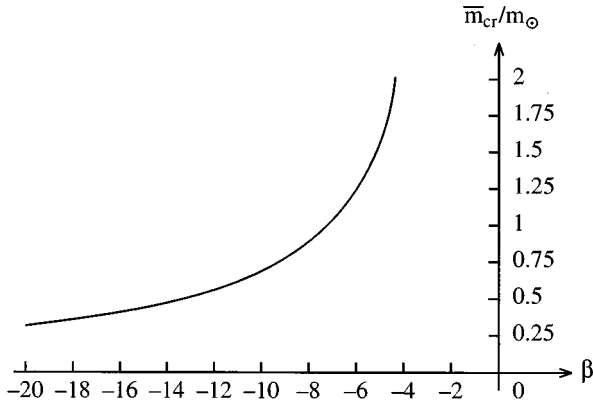


FIG. 2. Critical baryonic mass  $\bar{m}_{cr}$  versus the curvature parameter  $\beta$  within the quadratic models  $A(\varphi) = \exp(\frac{1}{2}\beta\varphi^2)$ .

which is the strong-field analogue of the quantity  $\beta_0 = \partial\alpha(\varphi_0)/\partial\varphi_0$  entering the Eddington parameter  $\beta_{\text{Edd}} - 1$ , Eq. (1.4b). The quantity  $\beta_A$  directly enters many observable orbital effects in binary-pulsar systems [5].

Summarizing, we conclude that the nonperturbative phenomenon discussed in [10] can be simply interpreted as a “spontaneous scalarization” phenomenon, i.e., a scalar analogue of ferromagnetism. The condition for this phenomenon to occur in actual neutron stars depends on the equation of state of neutron matter. For a polytropic model representing a realistic equation of state (with maximum baryonic mass of  $2.23m_{\odot}$  in general relativity), we found that the critical baryonic mass<sup>2</sup> for spontaneous scalarization is smaller than about  $1.5m_{\odot}$  (which corresponds to a general relativistic mass  $\approx 1.4m_{\odot}$ ) when  $\beta_0 \equiv \partial^2 \ln A(\varphi_0)/\partial\varphi_0^2 \leq -5$ . For such values of  $\beta_0$ , actual neutron stars observed in binary pulsars would develop strong scalar charges even in absence of external scalar solicitation [i.e., even if  $\alpha_0 = \alpha(\varphi_0) = 0$ ]. For values  $-5 \leq \beta_0 \leq -4$ , one can still obtain important deviations from general relativity if the cosmological value of  $\alpha_0$  saturates the present weak-field limit (1.6). In all cases, the presence of a nonzero external  $\alpha_0$  smoothes the phase transition and leads to continuously (but fast) varying values of the effective coupling parameters  $\alpha_A$  and  $\beta_A$  as functions of the mass. Figure 2 displays the dependence  $\bar{m}_{cr}(\beta)$  for the quadratic model (2.1). Some representative numerical values are quoted in Table I. For  $\beta_0$  above some critical value  $\beta_{cr} \approx -4.34$ , the maximum mass is reached before the zero mode can develop. It is plausible (but difficult to confirm numerically) that as  $\beta \rightarrow \beta_{cr}$ , the critical baryonic mass tends to the general relativistic maximum baryonic mass ( $\approx 2.23m_{\odot}$  in our polytropic model).

The behavior discussed above concerns the scalar models invariant under the reflection symmetry  $\varphi \rightarrow -\varphi$ , such as  $A(\varphi) = \exp(\frac{1}{2}\beta\varphi^2)$  or  $A(\varphi) = \cos(\sqrt{-\beta}\varphi)$ . A dissymmetric

TABLE I. Critical baryonic mass  $\bar{m}_{cr}$  (and critical Einstein mass  $m_{cr}$ ) for some values of the curvature parameter  $\beta$  within the quadratic models  $A(\varphi) = \exp(\frac{1}{2}\beta\varphi^2)$ .

| $\beta$ | $\bar{m}_{cr}/m_{\odot}$ | $m_{cr}/m_{\odot}$ |
|---------|--------------------------|--------------------|
| -10     | 0.69                     | 0.66               |
| -9      | 0.78                     | 0.74               |
| -8      | 0.89                     | 0.84               |
| -7      | 1.04                     | 0.98               |
| -6      | 1.24                     | 1.16               |
| -5.5    | 1.38                     | 1.28               |
| -5      | 1.56                     | 1.43               |
| -4.5    | 1.84                     | 1.65               |
| -4.35   | 2.01                     | 1.78               |

coupling function, such as  $A(\varphi) = \exp(\frac{1}{2}\beta\varphi^2 + \frac{1}{6}\beta'\varphi^3)$ , would lead to hysteresis phenomena (first-order rather than second-order phase transition): For some values of the control parameter  $\bar{m}_A$ , there will be two locally stable energy minima available. The scalar configuration chosen by the star would depend on the route taken to evolve into its present mass state. Let us also mention that we would get an even richer (Goldstone-like) phenomenology if we were to consider models involving several scalar fields, with, e.g., spontaneous breaking of a continuous symmetry in the scalar-field space. Finally, let us make it clear that a negative value for  $\beta_0 \equiv \partial^2 \ln A/\partial\varphi_0^2$  does not mean at all that we are introducing some pathology in our scalar-field model. The theories we consider are well-behaved field models having only positive-energy excitations. A negative value of  $\beta_0$  means only that scalar field nonlinearities can reinforce the naturally attractive character of scalar interactions, so that it becomes energetically favorable to generate more scalar-field energy.<sup>3</sup>

### III. SLOWLY ROTATING NEUTRON STARS IN TENSOR-SCALAR GRAVITY

One of the main objects of the present paper is to show how to compute the moments of inertia of slowly rotating neutron stars in tensor-scalar gravity, especially in the presence of the nonperturbative strong-scalar-field effects recalled above. We shall work in the Einstein conformal frame, within which the basic global mechanical quantities, such as total mass and total angular momentum, are conserved (in absence of radiation or particle exchange) and can, as usual, be read off the asymptotic expansion of the metric. The total

<sup>2</sup>Note that one can determine the critical baryonic mass as a function of  $\beta$ , in the quadratic model (2.1), by solving a linear problem. Indeed, the onset of the transition happens when Eq. (1.2b) with  $\alpha(\varphi) = \beta\varphi$  (and  $g_*$  and  $T_*$  replaced by a background general relativistic solution) first admits a “zero mode,” i.e., a nontrivial homogeneous solution with vanishing boundary conditions [10].

<sup>3</sup>The appearance of a negative critical value of  $\beta_0$  can be easily understood in the lowest approximation, where the scalar energy functional to be minimized reads (when setting  $G=c=1$ )  $E[\varphi] = \int d^3x [ (1/8\pi)(\partial_i\varphi)^2 + \rho(1 + \frac{1}{2}\beta\varphi^2) ]$ . Indeed, let us consider for instance the simplest trial continuous field configurations,  $\varphi(r) = \text{const} = \omega_A/R$  inside a star of mass  $m = \int d^3x \rho$  and  $\varphi(r) = \omega_A/r$  outside the star ( $r > R$ ). This yields  $E[\omega_A] = m + \frac{1}{2}C\omega_A^2$ , where  $C = R^{-1}(1 + \beta m/R)$  becomes negative for a sufficiently negative  $\beta$ . The missing stabilizing contribution  $+ \frac{1}{4}b\omega_A^4$  would come from taking into account higher-order nonlinearities.

mass  $m_A$  (in Einstein units) can be read off the  $1/r$  behavior of  $g_{00}^*$  or  $g_{ij}^*$ , while the  $z$  component of the total angular momentum  $J_A$  (in Einstein units) can be read off the  $1/r^2$  behavior of the mixed component  $g_{0i}^*$ . We consider only stationary axisymmetric field configurations. It has been shown by Hartle [13] (see also [14]) that the metric corresponding to a slowly rotating star could be written, when keeping only first-order terms in the angular velocity  $\Omega = u^\phi/u^t$ , as

$$ds_*^2 = g_{\mu\nu}^* dx^\mu dx^\nu = -e^{\nu(\rho)} c^2 dt^2 + e^{\mu(\rho)} d\rho^2 + \rho^2 d\theta^2 + \rho^2 \sin^2 \theta (d\phi + [\omega(\rho, \theta) - \Omega] dt)^2. \quad (3.1)$$

Thanks to the neglect of fractional corrections of order  $\Omega^2$ , the diagonal metric coefficients  $\nu(\rho)$  and  $\mu(\rho)$  can be taken to be the solutions corresponding to a spherically symmetric nonrotating star. The only new field variable which appears in the slowly rotating case is the function  $\omega(\rho, \theta)$  entering the mixed component  $g_{t\phi}^* = \rho^2 \sin^2 \theta [\omega(\rho, \theta) - \Omega]$ . The subtraction of the star's angular velocity  $\Omega$  is chosen for later convenience.<sup>4</sup> The total angular momentum  $J_A$  is read off the  $1/\rho^3$  behavior of  $\omega$ :

$$\omega = \Omega - \frac{G_*}{c^2} \frac{2J_A}{\rho^3} + O\left(\frac{1}{\rho^4}\right). \quad (3.2)$$

Then the inertia moment (in Einstein units) is defined, in the slow rotation limit, as the ratio

$$I_A = \frac{J_A}{\Omega} + O(\Omega^2). \quad (3.3)$$

We need now to write down explicitly the field equations (1.2). As the scalar field  $\varphi$  does not couple linearly to the rotation, the field equation for  $\varphi$  is, modulo terms of order  $\Omega^2$ , the same as for a spherically symmetric, nonrotating star [therefore  $\varphi$  will, modulo  $O(\Omega^2)$ , be spherically symmetric]. The field equation for the new variable  $\omega$  comes from

$$R_{*\phi}^t = 2\partial_\phi \varphi g_{*\alpha}^t \partial_\alpha \varphi + \frac{8\pi G_*}{c^4} T_{*\phi}^t. \quad (3.4)$$

Simply from axisymmetry ( $\partial_\phi = 0$ ) we see that the scalar contribution to the right-hand side of Eq. (3.4) vanishes exactly. We are then left with the usual Einstein field equations with a localized material source. Taking as usual a perfect fluid description of nuclear matter (with energy density  $\epsilon_*$  and pressure  $p_*$  in Einstein units) we can directly use the results of Refs. [13,14]. (One must, however, be careful not to use equations where the ‘‘diagonal’’ Einstein field equations have been replaced.) We find the following homogeneous equation for  $\omega$ :

<sup>4</sup>With this definition of variables, the stress-energy tensor of the fluid gives simply  $T_{*\phi}^t = (\epsilon_* + p_*) e^{-\nu} \rho^2 \omega \sin^2 \theta$  thanks to a combination between  $g_{t\phi}^*$  and  $\Omega = u^\phi/u^t$ .

$$\begin{aligned} & \frac{1}{\rho^4} \partial_\rho [\rho^4 e^{-(\nu+\mu)/2} \partial_\rho \omega] + \frac{e^{(\mu-\nu)/2}}{\rho^2 \sin^3 \theta} \partial_\theta (\sin^3 \theta \partial_\theta \omega) \\ &= \frac{16\pi G_*}{c^4} (\epsilon_* + p_*) e^{(\mu-\nu)/2} \omega. \end{aligned} \quad (3.5)$$

As in Refs. [13,14], a decomposition of  $\omega(\rho, \theta)$  in associated Legendre polynomials  $dP_\ell(\cos \theta)/d\cos \theta$  shows that there is only a  $P$  contribution ( $\ell=1$ ), so that, in fact,  $\omega$  depends only on  $\rho$  and not on  $\theta$ . Adding the scalar-modified diagonal Einstein equations (written in [10]), we finally get the following complete set of radial equations for our field variables (a prime denoting  $d/d\rho$ ):

$$M' = \frac{4\pi G_*}{c^4} \rho^2 A^4(\varphi) \bar{\epsilon} + \frac{1}{2} \rho(\rho - 2M) \psi^2, \quad (3.6a)$$

$$\nu' = \frac{8\pi G_*}{c^4} \frac{\rho^2 A^4(\varphi) \bar{p}}{\rho - 2M} + \rho \psi^2 + \frac{2M}{\rho(\rho - 2M)}, \quad (3.6b)$$

$$\varphi' = \psi, \quad (3.6c)$$

$$\begin{aligned} \psi' &= \frac{4\pi G_*}{c^4} \frac{\rho A^4(\varphi)}{\rho - 2M} [\alpha(\varphi)(\bar{\epsilon} - 3\bar{p}) + \rho \psi(\bar{\epsilon} - \bar{p})] \\ &\quad - \frac{2(\rho - M)}{\rho(\rho - 2M)} \psi, \end{aligned} \quad (3.6d)$$

$$\begin{aligned} \bar{p}' &= -(\bar{\epsilon} + \bar{p}) \left[ \frac{4\pi G_*}{c^4} \frac{\rho^2 A^4(\varphi) \bar{p}}{\rho - 2M} + \frac{1}{2} \rho \psi^2 \right. \\ &\quad \left. + \frac{M}{\rho(\rho - 2M)} + \alpha(\varphi) \psi \right], \end{aligned} \quad (3.6e)$$

$$\bar{M}' = 4\pi \tilde{m}_b \tilde{n} A^3(\varphi) \frac{\rho^2}{\sqrt{1 - 2M/\rho}}, \quad (3.6f)$$

$$\omega' = \varpi, \quad (3.6g)$$

$$\begin{aligned} \varpi' &= \frac{4\pi G_*}{c^4} \frac{\rho^2}{\rho - 2M} A^4(\varphi) (\bar{\epsilon} + \bar{p}) \left( \varpi + \frac{4\omega}{\rho} \right) \\ &\quad + \left( \psi^2 \rho - \frac{4}{\rho} \right) \varpi. \end{aligned} \quad (3.6h)$$

The notation used in Eqs. (3.6) is the following:  $M(\rho)$  is defined by writing the radial metric coefficient  $g_{\rho\rho}$  as  $e^{\mu(\rho)} \equiv [1 - 2M(\rho)/\rho]^{-1}$ . As usual the value of  $M(\rho)$  at infinity is the total Arnowitt-Deser-Misner (ADM) mass. The fluid variables have been expressed in physical units using  $T_{*\mu}^\nu = A^4(\varphi) \tilde{T}_\mu^\nu$ . [It is in these units that one can write a usual equation of state  $\bar{\epsilon} = \bar{\epsilon}(\tilde{n})$ ,  $\bar{p} = \bar{p}(\tilde{n})$ , where  $\tilde{n}$  denotes the physical number density of baryons.]  $\psi$  and  $\varpi$  are just intermediate notations for the radial derivatives of  $\varphi$  and  $\omega$ , respectively. Finally, we have added an equation for the radial distribution of the baryonic mass  $\bar{m}_A = \bar{M}(R) = \tilde{m}_b \int_A \tilde{n} \sqrt{\tilde{g}} \tilde{u}^0 d^3x = \tilde{m}_b \int_0^R 4\pi \tilde{n} A^3(\varphi) \rho^2 (1 - 2M/\rho)^{-1/2} d\rho$ , where  $R$  denotes the (Schwarzschild-coordinate) radius of the star (i.e., the value of  $\rho$  where  $\bar{p}$  and  $\bar{\epsilon}$  vanish).



Note that several of the right-hand sides of Eqs. (3.6) contain terms proportional to  $\psi^2 = (\varphi')^2$  (i.e., proportional to the scalar-field energy density). These terms do not vanish outside the star. However, one can avoid numerically integrating Eqs. (3.6) up to  $\rho = \infty$  by matching the result of integrating them up to the radius  $R$  of the star to the known general form of the exact static, spherically symmetric exterior solution. This is, however, a bit subtle because the general exterior solution can only be written in closed form in some special coordinates introduced by Just [15,16,5] or (through a simple transformation) in isotropic coordinates, but not in the Schwarzschild coordinates we are using. Still, it was shown in [10] how to extract, via a matching across the star's surface, the global quantities  $m_A$  and  $\alpha_A$  from the results of integrating Eqs. (3.6) up to  $\rho = R$ . We need to do here more work to extract  $J_A$  (and  $I_A$ ) from the results for the variables  $\omega$  and  $\varpi \equiv d\omega/d\rho$ .

Outside the star, Eq. (3.5) (with  $\partial_\theta = 0$ ) shows directly that  $\rho^4 e^{-(\nu+\mu)/2} \partial_\rho \omega$  is a constant. From Eq. (3.2), this constant is simply related to the total angular momentum, so that

$$\frac{d\omega}{d\rho} = 6 \frac{G_*}{c^2} J_A \frac{e^{(\nu+\mu)/2}}{\rho^4} \quad (\text{outside the star}). \quad (3.7)$$

Equation (3.7) gives one equation to determine  $J_A$ . We need another equation to determine  $\Omega$  and then  $I_A \equiv J_A/\Omega$ . Note that the equation for  $\omega$  [e.g., Eq. (3.5)] is homogeneous in  $\omega$ . Therefore, we can start the radial integration with an arbitrary (nonzero) value of  $\omega(\rho)$  at  $\rho = 0$ , but we need to extract from  $\omega(\rho)$  the value of the fluid angular velocity  $\Omega$  implied by this arbitrary choice. To achieve this, it suffices to integrate explicitly Eq. (3.7) with the boundary condition  $\omega(\rho) \rightarrow \Omega$  when  $\rho \rightarrow \infty$  [as is clear from Eqs. (3.1) or (3.2)]. This integration can be done by rewriting Eq. (3.7) in Just radial coordinate  $r$ . Indeed, the general exterior static, spherically symmetric solution [15,16,5] reads

$$ds_*^2 = -e^\nu c^2 dt^2 + e^{-\nu} [dr^2 + (r^2 - ar)(d\theta^2 + \sin^2 \theta d\phi^2)], \quad (3.8a)$$

$$e^{\nu(r)} = \left(1 - \frac{a}{r}\right)^{b/a}, \quad (3.8b)$$

$$\varphi(r) = \varphi_0 + \frac{d}{a} \ln \left(1 - \frac{a}{r}\right), \quad (3.8c)$$

where the integration constants  $a, b, d$  are constrained by  $a^2 - b^2 = 4d^2$ , and are expressible in terms of the total Einstein mass  $m_A$  and the effective coupling constant  $\alpha_A$ , Eq. (2.3), via

$$b = 2 \frac{G_*}{c^2} m_A, \quad (3.9a)$$

$$\frac{a}{b} = \sqrt{1 + \alpha_A^2}, \quad (3.9b)$$

$$\frac{d}{b} = \frac{1}{2} \alpha_A. \quad (3.9c)$$

Comparing Eq. (3.8a) with the Schwarzschild form (3.1) yields

$$\rho = r \left(1 - \frac{a}{r}\right)^{(a-b)/2a}, \quad (3.10a)$$

$$e^\mu = \left(1 - \frac{a}{r}\right) \left(1 - \frac{a+b}{2r}\right)^{-2}. \quad (3.10b)$$

Inserting these results into Eq. (3.7) leads to an elementary integral for  $\omega(r)$ . To write explicitly the answer it is convenient to introduce the parameter

$$p \equiv \frac{1}{a} \ln \left(1 - \frac{a}{r}\right). \quad (3.11)$$

In terms of  $p$ , the exact exterior solution for  $\omega$  reads

$$\begin{aligned} \omega = \Omega + \frac{6G_* J_A}{c^2 b (4b^2 - a^2)} & \left\{ e^{2bp} - 1 + e^{2bp} \right. \\ & \times \left[ \left( \frac{2b}{a} \right)^2 [\cosh(ap) - 1] - \frac{2b}{a} \sinh(ap) \right] \Big\}. \end{aligned} \quad (3.12)$$

Combining the results just derived on the radial dependence of  $\omega$  with the results of [10] for the matching of the other field variables, we can finally write a set of equations allowing one to extract all the needed physical quantities from the surface values obtained from integrating Eqs. (3.6) from the center  $\rho = 0$ :

$$R \equiv \rho_s, \quad (3.13a)$$

$$\nu'_s \equiv R \psi_s^2 + \frac{2M_s}{R(R - 2M_s)}, \quad (3.13b)$$

$$\alpha_A \equiv \frac{2\psi_s}{\nu'_s}, \quad (3.13c)$$

$$Q_1 \equiv (1 + \alpha_A^2)^{1/2}, \quad (3.13d)$$

$$Q_2 \equiv (1 - 2M_s/R)^{1/2}, \quad (3.13e)$$

$$\hat{\nu}_s \equiv -\frac{2}{Q_1} \operatorname{arctanh} \left( \frac{Q_1}{1 + 2(R\nu'_s)^{-1}} \right), \quad (3.13f)$$

$$\varphi_0 \equiv \varphi_s - \frac{1}{2} \alpha_A \hat{\nu}_s, \quad (3.13g)$$

$$\frac{G_*}{c^2} m_A \equiv \frac{1}{2} \nu'_s R^2 Q_2 \exp \left( \frac{1}{2} \hat{\nu}_s \right), \quad (3.13h)$$

$$\bar{m}_A \equiv \bar{M}_s, \quad (3.13i)$$

$$\frac{G_*}{c^2} J_A \equiv \frac{1}{6} \varpi_s R^4 Q_2 \exp \left( -\frac{1}{2} \hat{\nu}_s \right), \quad (3.13j)$$

$$\Omega \equiv \omega_s - \frac{c^4}{G_*^2} \frac{3J_A}{4m_A^3(3-\alpha_A^2)} \left\{ e^{2\hat{\nu}_s} - 1 + \frac{4G_*m_A}{Rc^2} e^{\hat{\nu}_s} \right. \\ \left. \times \left[ \frac{2G_*m_A}{Rc^2} + e^{\hat{\nu}_s/2} \cosh\left(\frac{1}{2}Q_1\hat{\nu}_s\right) \right] \right\}, \quad (3.13k)$$

$$I_A \equiv \frac{J_A}{\Omega}. \quad (3.13l)$$

The notation used in Eqs. (3.13) is that a suffix  $s$  denotes the surface value of any of the variables entering the first-order system (3.6). The only exception [apart from  $\nu'_s$ , which we redefine explicitly as the surface value of the right-hand side of Eq. (3.6b)] is  $\hat{\nu}_s$ , which is the “correct” value of  $\nu$  at the surface when  $\nu$  is normalized as being zero at infinity. Indeed, as the system (3.6) is integrated from the center [starting with an arbitrary value of  $\nu(0)$ ] up to the surface, the surface value of  $\nu(\rho)$  naively obtained from integrating Eqs. (3.6) is not the one to be used in any of the physically normalized results.

Let us finally mention the set of initial conditions, at the center, used for integrating Eqs. (3.6). Actually, because of the singular nature of the point  $\rho=0$ , one numerically imposes initial conditions at a small but nonzero radius  $\rho_{\min}$ . The values of some of the radial derivatives ( $\varphi' \equiv \psi$  and  $\omega' \equiv \varpi$ ) are determined so as to be consistent with regular Taylor expansions at the origin [for instance, writing  $\varphi(\rho) = \varphi(\mathbf{x}) = \varphi(\mathbf{0}) + \frac{1}{6}\mathbf{x}^2\Delta\varphi(\mathbf{0}) + O(\mathbf{x}^4)$  determines  $\varphi'(\rho) \sim \frac{1}{3}\rho\Delta\varphi(0)$  as  $\rho \rightarrow 0$ ]. The complete set of initial conditions reads

$$M(\rho_{\min}) = 0, \quad (3.14a)$$

$$\nu(\rho_{\min}) = 0, \quad (3.14b)$$

$$\varphi(\rho_{\min}) = \varphi_c, \quad (3.14c)$$

$$\psi(\rho_{\min}) = \left(\frac{1}{3}\rho_{\min}\right) \frac{4\pi G_*}{c^4} A^4(\varphi_c) \alpha(\varphi_c) [\tilde{\epsilon}(\tilde{n}_c) - 3\tilde{p}(\tilde{n}_c)], \quad (3.14d)$$

$$\tilde{n}(\rho_{\min}) = \tilde{n}_c, \quad (3.14e)$$

$$\bar{M}(\rho_{\min}) = 0, \quad (3.14f)$$

$$\omega(\rho_{\min}) = 1, \quad (3.14g)$$

$$\varpi(\rho_{\min}) = \left(\frac{1}{5}\rho_{\min}\right) \frac{16\pi G_*}{c^4} A^4(\varphi_c) [\tilde{\epsilon}(\tilde{n}_c) + \tilde{p}(\tilde{n}_c)] \omega(\rho_{\min}). \quad (3.14h)$$

Note that (as discussed above) the initial conditions (3.14b) and (3.14g) are arbitrary, and that we transform Eq. (3.6e) in an evolution equation for the physical number density  $\tilde{n}$  using the equation of state, i.e.,  $\tilde{p}' = (d\tilde{p}(\tilde{n})/d\tilde{n}) \times \tilde{n}'$ . The choice of  $\varphi_c$  and  $\tilde{n}_c$  is discussed below.

#### IV. GRAVITATIONAL FORM FACTORS OF ROTATING NEUTRON STARS

##### A. Scalar-field dependence of the inertia moment

Extending the analysis of [10], we have studied the impact of scalar-induced strong-field effects on the gravitational form factors of neutron stars. By “gravitational form factor” we mean the set of coupling constants that appear, within tensor-scalar theories, in the description of the relativistic motion and timing of binary (and isolated) pulsars. As discussed in detail<sup>5</sup> in [5], the  $(v/c)^2$ -accurate orbital dynamics of binary systems depends, besides the Einstein masses of the two objects  $m_A$  and  $m_B$ , on the effective scalar coupling constants  $\alpha_A, \alpha_B$ , defined in Eq. (2.3), as well as on their scalar-field derivatives  $\beta_A, \beta_B$ , Eq. (2.4). It was also shown in [5] that the same parameters  $\alpha_A, \alpha_B, \beta_A, \beta_B$  suffice to express all radiation reaction effects [up to  $O(v^7/c^7)$ ] in a tensor-scalar description of compact binary systems. On the other hand, the relativistic timing of binary-pulsar systems involves, besides the above  $\alpha$ ’s and  $\beta$ ’s, a new parameter describing the possible field dependence of the inertia moment  $I_A$  of the pulsar. [In the following, we use the label  $A$  to indicate the timed pulsar, by opposition to the companion labeled  $B$ .] Indeed, as pointed out by Eardley [17] (see also [18]), the adiabatic invariance (under the slow variation of the local scalar-field environment caused by the motion of the companion) of the total angular momentum of the pulsar  $J_A = I_A(\varphi_{0A}^{\text{loc}})\Omega_A$  implies that the angular velocity of the pulsar  $\Omega_A$  will fluctuate in response to the orbital-induced variations of the external scalar field  $\varphi_{0A}^{\text{loc}}$  locally felt by the pulsar. As discussed in more detail below, the observable deviations from general relativity implied by this effect are given by the parameter  $K_A^B \equiv -\alpha_B \partial \ln I_A / \partial \varphi_0$ , in which  $I_A$  denotes, as above, the inertia moment of the pulsar in (local) Einstein units.

To compute  $\partial \ln I_A / \partial \varphi_0$ , we have numerically integrated Eqs. (3.6) with a suitable “shooting” strategy for the choice of initial conditions. Indeed, the quantities that are physically fixed are  $\varphi_0$  (the value of  $\varphi$  far from the star) and  $\bar{m}_A$  (the baryonic mass of the neutron star). [Note that when a derivative with respect to  $\varphi_0$  is taken, as in the definitions of  $\beta_A$ , Eq. (2.4), or of  $K_A^B$ , it must be performed for a fixed value of  $\bar{m}_A$ .] Therefore, by trial and error, one must vary the initial conditions  $\varphi_c$  and  $\tilde{n}_c$  in Eqs. (3.14) until they lead to the desired values of  $\varphi_0$  and  $\bar{m}_A$ . In the end, one wants to explore the way the observables  $m_A, \alpha_A, \beta_A, I_A, \partial \ln I_A / \partial \varphi_0, \dots$  depend upon  $\varphi_0$  and  $\bar{m}_A$ .

The values of  $m_A, \alpha_A, \dots$  as functions of  $\varphi_0$  and  $\bar{m}_A$  depend upon the equation of state used to describe the nuclear matter in the neutron star. We shall discuss in a later publication the dependence of our results on the choice of the equation of state. In the present work, we shall consider, for simplicity, only a fixed polytropic equation of state:

$$\tilde{\epsilon} = \tilde{n} \tilde{m}_b + \frac{K \tilde{n}_0 \tilde{m}_b}{\Gamma - 1} \left( \frac{\tilde{n}}{\tilde{n}_0} \right)^\Gamma, \quad (4.1a)$$

<sup>5</sup>We restrict here the more general results of [5] to the simple case where there is only one scalar field.

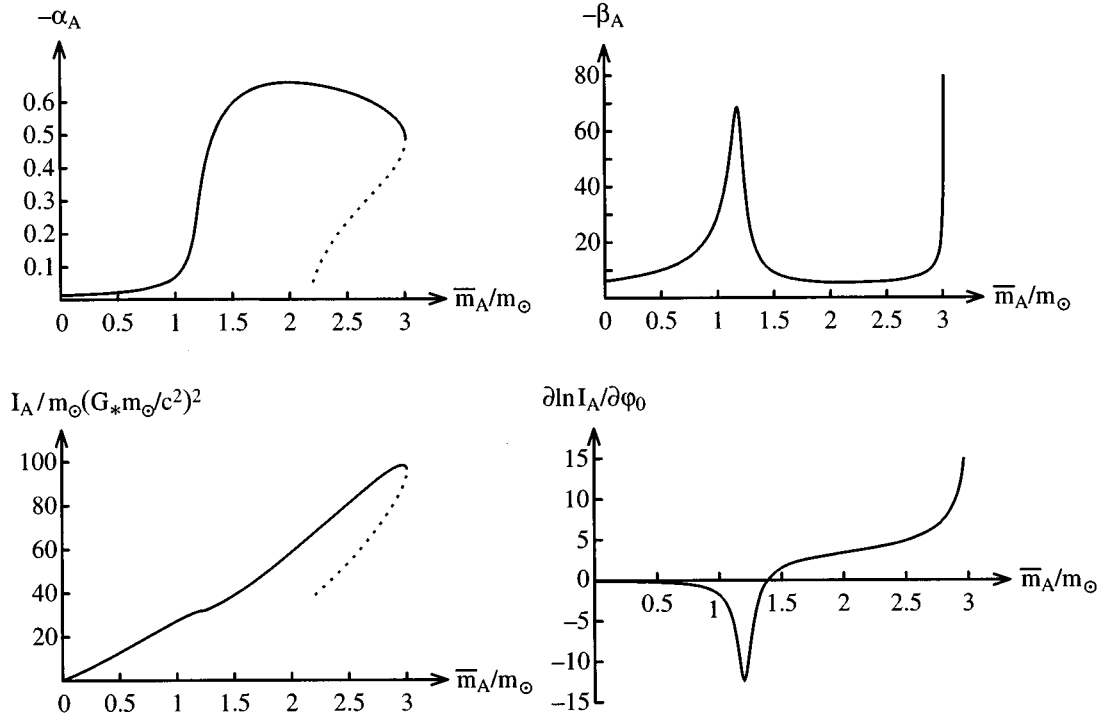


FIG. 3. Dependence upon the baryonic mass  $\bar{m}_A$  of the coupling parameters  $\alpha_A$ ,  $\beta_A$ , the inertia moment  $I_A$ , and its derivative  $\partial \ln I_A / \partial \varphi_0$ . These plots correspond to the model  $A(\varphi) = \exp(-3\varphi^2)$  and the maximum value of  $\varphi_0$  allowed by solar-system experiments. As in Fig. 1, the dotted lines correspond to unstable configurations of the star.

$$\tilde{p} = K \tilde{n}_0 \tilde{m}_b \left( \frac{\tilde{n}}{\tilde{n}_0} \right)^\Gamma. \quad (4.1b)$$

All quantities in Eqs. (4.1) are in local physical units;  $\tilde{m}_b \equiv 1.66 \times 10^{-24}$  g is a fiducial baryon mass and  $\tilde{n}_0 \equiv 0.1 \text{ fm}^{-3}$  a typical nuclear number density. We shall use the following specific values of the polytropic parameters  $\Gamma$  and  $K$ :

$$\Gamma = 2.34, \quad K = 0.0195, \quad (4.2)$$

which have been chosen to fit a realistic equation of state which is neither too hard nor too soft: the equation of state II of Ref. [12]. (The polytropic constant  $K$  should not be confused with the parameter  $K_A^B$  linked to the scalar-field-induced variation of the inertia moment.) The precise values (4.2) were adjusted to fit the curve giving, in general relativity, the fractional binding energy  $f \equiv (\bar{m} - m)/m$  as a function of the baryonic mass. In particular they lead to the same maximum baryonic mass  $\bar{m}_{\text{max}} = 2.23 m_\odot$  in general relativity. Let us note in passing that to convert from the nuclear fiducial quantities to more adequate astrophysical units ( $m_\odot$  for masses,  $G_* m_\odot / c^2$  for distances), it is convenient to use the numerical value

$$\frac{4 \pi G_* \tilde{n}_0 \tilde{m}_b}{c^2} \left( \frac{G_* m_\odot}{c^2} \right)^2 = \frac{1}{296.135}. \quad (4.3)$$

For technical convenience, when comparing different theories we keep fixed  $G_* = 6.67 \times 10^{-8} \text{ cm}^3 \text{ g}^{-1} \text{ s}^{-2}$  (and  $m_\odot = 1.99 \times 10^{33}$  g, measured in  $g^*$  units). See Ref. [5] for

the factors (differing from unity by  $\lesssim 10^{-3}$ ) relating  $g^*$ -frame quantities to directly observable ones.

We present in Fig. 3 some of our numerical results for the dependence upon the baryonic mass of  $\alpha_A$ ,  $\beta_A$ ,  $I_A$  [in units of  $m_\odot (G_* m_\odot / c^2)^2$ ] and  $\partial \ln I_A / \partial \varphi_0$ . All the results of these figures have been computed within the tensor-scalar theory defined by the particular coupling function

$$A_{\bar{\phi}}(\varphi) \equiv \exp(-3\varphi^2). \quad (4.4)$$

This model belongs to the class of quadratic models (2.1), and possesses a curvature parameter for the logarithm of the coupling function,  $\beta = \beta_0 = \partial^2 \ln A / \partial \varphi_0^2 = -6$ . In the limit where  $\varphi_0 \rightarrow 0$ , this model exhibits a spontaneous scalarization above a critical baryonic mass  $\bar{m}_{\text{cr}} = 1.24 m_\odot$ . As explained in Sec. II, the presence of a nonzero external scalar background  $\varphi_0 \neq 0$  smoothes the scalarization and leads to continuous variations of  $\alpha_A, \beta_A, \dots$  as functions of  $\bar{m}_A$ . For instance, instead of having a Curie-type blowup  $\propto |\bar{m}_A - \bar{m}_{\text{cr}}|^{-1}$  for the zero-external-field “susceptibility”  $\beta_A = \partial \alpha_A / \partial \varphi_0$ , we get a “resonance” bump in  $\beta_A$  when  $\bar{m}_A \approx \bar{m}_{\text{cr}}$ . There remains, however, an infinite blowup in  $\beta_A$  when  $\bar{m}_A$  reaches the maximum baryonic mass. It is easy to see analytically that this blowup must be there. (The same remark applies to  $\partial \ln I_A / \partial \varphi_0$ .) For definiteness, we have drawn Fig. 3 for the value

$$\varphi_0 = \varphi_0^{\text{max}} \equiv 2.4 \times 10^{-3}, \quad (4.5)$$

which is the maximum value of  $\varphi_0$  allowed by present weak-field tests within the model (4.4). This maximum value is



obtained from considering not only the limit  $\alpha_0^2 < 10^{-3}$ , Eq. (1.6), coming from time-delay and light-deflection experiments [8], but also the limit

$$|\beta_0| \alpha_0^2 < 1.2 \times 10^{-3}, \quad (4.6)$$

coming from the lunar-laser-ranging constraint  $|\bar{\beta}| < 6 \times 10^{-4}$  [19] on the Eddington parameter  $|\bar{\beta}| \equiv \beta_{\text{Edd}} - 1 \approx \frac{1}{2} \beta_0 \alpha_0^2$  [see Eq. (1.4b)]. When  $|\beta_0| > 1.2$ , the limit (4.6) is more stringent than the limit (1.6) and defines the maximal allowed value for  $|\alpha_0|$  and thereby for  $|\varphi_0| \approx |\alpha_0 / \beta_0|$  (see the exclusion plot in Sec. V D below).

Besides the variation of the shapes of the curves in Fig. 3 when  $\varphi_0$  is allowed to vary (which is always a sharpening of the bumps and a stabilization of the other features<sup>6</sup>), we have also numerically explored the effect of varying the curvature parameter  $\beta$  in Eq. (2.1). The two main effects of varying  $\beta$  are (i) to enlarge the values of the form factors  $|\alpha_A|$ ,  $|\beta_A|$ ,  $|\partial \ln I_A / \partial \varphi_0|$  as  $-\beta$  increases, and (ii) to displace the location of the critical point  $\bar{m}_{\text{cr}}$ . For instance, we find [within the models (2.1)]  $\bar{m}_{\text{cr}}(\beta = -5) = 1.56 m_\odot$ ,  $\bar{m}_{\text{cr}}(\beta = -4.5) = 1.84 m_\odot$ . These values are below the (expected) maximum mass of a neutron star. However, observed neutron stars have baryonic masses around  $1.5 m_\odot$  (corresponding to general relativistic Einstein masses around  $1.4 m_\odot$ ); therefore, we expect that strong-scalar-field effects can have significant observational consequences only when  $\beta \leq -5$ .

### B. Scalar-field effects in the timing parameter $\gamma$

Up to now, the non-Einsteinian effects linked to the field dependence of the inertia moment have been treated by an approximation [17,18,5] which is insufficient for tackling the nonperturbative phenomena discussed here. One of the main aims of the present paper is to remedy this situation. Let us first clarify the observable effect of the variation of the pulsar inertia moment with the local scalar background<sup>7</sup>  $\varphi_A \equiv \varphi_{0A}^{\text{loc}}$  [17,18].

The central tool of binary-pulsar experiments is the “timing formula” (see, e.g., [20,21]), i.e., the mathematical function relating the “intrinsic time” of the pulsar clock  $T$  to the arrival time on Earth of radio pulses. The successive ticks of the pulsar time  $T$  are defined to correspond to successive  $2\pi$  rotations of the pulsar around itself:  $\phi^{\text{PSR}} = 2\pi T / P_p$ , where  $P_p$  is the intrinsic period of the pulsar (for simplicity we neglect here the slowdown of the rotation of the pulsar as well as aberration effects). In other words, adding the label  $A$  and passing to a differential formulation,  $dT_A = C d\phi_A$  for a certain constant  $C$ . In (local) Einstein units, the pulsar angular momentum reads  $J_A = I_A \Omega_A = I_A d\phi_A / d\tau_A^*$ , where  $d\tau_A^* = |ds_A^*|/c = (-g_{\mu\nu}^* dz_A^\mu dz_A^\nu)^{1/2}/c$  is the Einstein proper time in a local inertial frame around  $A$ . The angular momen-

tum  $J_A$  is an action variable [ $J = p_\phi = (1/2\pi) \oint p_i dq^i$ ] and therefore an adiabatic invariant under slow changes of parameters. It remains therefore constant as the pulsar moves on its orbit and feels a slowly changing  $\varphi_A$  from its companion. This yields  $dT_A = C' d\tau_A^* / I_A$  for some new constant  $C'$ . The latter equation can be approximately rewritten in terms of some coordinate time  $t$  used to describe the binary motion:

$$dT_A \approx C' \sqrt{-g_{00}^*} \sqrt{1 - \mathbf{v}_A^2 / c^2} dt / I_A(\varphi_A(t)), \quad (4.7)$$

where (to sufficient accuracy)  $\mathbf{v}_A^2$  is the Euclidean square of the coordinate velocity of the pulsar  $\mathbf{v}_A = d\mathbf{z}_A / dt$ . Using (see [5])

$$\sqrt{-g_{00}^*} = 1 - \frac{G_* m_B}{r_{AB} c^2} + O\left(\frac{1}{c^4}\right), \quad (4.8a)$$

$$\varphi_A(t) = \varphi_0 - \frac{G_* m_B \alpha_B}{r_{AB} c^2} + O\left(\frac{1}{c^4}\right), \quad (4.8b)$$

and the standard relations given by Newtonian orbital dynamics [with effective Newtonian constant  $G_{AB} = G_*(1 + \alpha_A \alpha_B)$ ], we find a usual “Einstein” contribution  $\Delta_E = \gamma \sin u$  to the timing formula [20,21]. In  $\Delta_E$ ,  $u$  denotes the function of  $T_A$  defined by solving  $u - e \sin u = 2\pi[(T_A - T_0)/P_b - \frac{1}{2} \dot{P}_b ((T_A - T_0)/P_b)^2]$ , and<sup>8</sup>

$$\gamma \equiv \gamma^{\text{th}}(m_A, m_B) = \frac{e}{n} \frac{X_B}{1 + \alpha_A \alpha_B} \left( \frac{G_{AB}(m_A + m_B)n}{c^3} \right)^{2/3} \times [X_B(1 + \alpha_A \alpha_B) + 1 + K_A^B]. \quad (4.9)$$

The timing parameter  $\gamma$  should not be confused with the Eddington parameter  $\gamma_{\text{Edd}}$ . Here  $e$  is the orbital eccentricity,  $n \equiv 2\pi/P_b$  the orbital circular frequency,  $X_B \equiv m_B / (m_A + m_B)$ , and the new contribution  $K_A^B$  coming from the variation of  $I_A$  under the influence of the companion  $B$  is defined by

$$K_A^B \equiv -\alpha_B \frac{\partial \ln I_A}{\partial \varphi_0}. \quad (4.10)$$

Note the dissymmetric roles of the labels  $A$  and  $B$ . It is important, for applications, to recognize that the dependence of the correction  $K_A^B$  upon the two masses  $m_A, m_B$  is factorized (in the single scalar case that we consider here). Accordingly, it might be convenient to define the quantity

$$k_A(m_A) \equiv -\partial \ln I_A / \partial \varphi_0, \quad (4.11)$$

so that  $K_A^B(m_A, m_B) = k_A(m_A) \alpha_B(m_B)$ .

The reasoning above (based on the use of the Einstein conformal frame) could be done using the “physical” (or Jordan-Fierz) conformal frame. Indeed, the angular momentum is independent of the conformal frame (being an *action* variable). This means  $I_A \Omega_A = \tilde{I}_A \tilde{\Omega}_A$  so that the pulsar intrinsic time (which is a conformal invariant, being proportional

<sup>6</sup>See, for instance, Fig. 1 above which shows that the wide plateau in  $\alpha_A$ , beyond  $\bar{m}_{\text{cr}}$ , varies very little when  $\varphi_0$  tends to zero.

<sup>7</sup>This denotes the nearly uniform value of  $\varphi$  on a sphere centered on  $A$  having a radius much larger than the radius of the neutron star  $A$  but much smaller than the distance to the companion.

<sup>8</sup>The notation  $\gamma^{\text{th}}(m_A, m_B)$  in Eq. (4.9) refers to the theoretical prediction, within tensor-scalar models, giving the phenomenological timing parameter  $\gamma$  as a function of the masses. See below.

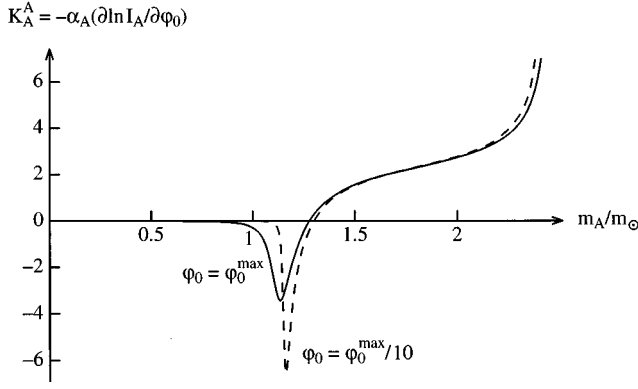


FIG. 4. Parameter  $K_A^A = -\alpha_A(\partial \ln I_A / \partial \varphi_0)$  versus the Einstein inertial mass  $m_A$ , within the model  $A(\varphi) = \exp(-3\varphi^2)$ . The solid line corresponds to the maximum value of  $\varphi_0$  allowed by solar-system experiments, and the dashed line to a tenfold smaller value of  $\varphi_0$  (i.e., a 100 times smaller value of the Eddington parameter  $\gamma_{\text{Edd}} - 1$ ).

to the angle  $\phi_A$ ) can be equivalently written as<sup>9</sup>  $dT_A = C' d\tau_A^*/I_A = C' d\tilde{\tau}_A/\tilde{I}_A$ . The calculation is (as always) slightly more complicated in the Jordan-Fierz frame and leads to a correction  $\tilde{K}_A^B$  instead of the  $K_A^B$  in Eq. (4.9), given by the sum of two terms:  $\tilde{K}_A^B = \alpha_0 \alpha_B - \alpha_B \partial \ln \tilde{I}_A / \partial \varphi_0$ , which is (as it should) found to be identically equal to  $K_A^B$ , Eq. (4.10), when using the link  $\tilde{I}_A = A(\varphi_A) I_A$ .

In previous works [17,18,5] one had assumed, as an approximation, that  $\tilde{I}_A$  was simply a function of the local, externally imposed, value of the effective gravitational “constant”  $\tilde{G}(\varphi_A)$ . Such an assumption is meaningful only in a “quasi-weak-field” approximation where one formally considers the compactness of a neutron star as a small expansion parameter (see Sec. 8.1 of [5]). This approximation breaks down precisely when the strong-scalar-field effects studied here develop (i.e., when  $|\beta| \gtrsim 4$ ). Previous treatments introduced the parameter  $\kappa_A \equiv -\partial \ln \tilde{I}_A / \partial \ln \tilde{G}_A$ . When it is meaningfully defined, the parameter  $\kappa_A$  is linked to the parameter  $k_A \equiv -\partial \ln I_A / \partial \varphi_0$  introduced above by  $k_A \approx \alpha_0 + 2\alpha_0[1 + \beta_0/(1 + \alpha_0^2)]\kappa_A$ . This formula shows that, under the assumptions of previous approximate treatments, the correction  $K_A^B$  was proportional to the product  $\alpha_0 \alpha_B$  between the *weak-field* scalar coupling  $\alpha_0$  and the possibly strong-field amplified effective coupling  $\alpha_B$ . As  $\alpha_0$  is observationally strongly constrained, this led always to small values of  $K_A^B$  with nearly negligible observational effects. By contrast, the exact result (4.10) is fully sensitive to strong-scalar-field effects taking place both in the pulsar and its companion. To illustrate the order of magnitude of possible deviations from the general relativistic prediction<sup>10</sup> for the timing parameter  $\gamma$  in systems made of two neutron stars, we plot in Fig. 4 the value of  $K_A^A$  (corresponding to the cases where  $m_B = m_A$ ) versus  $m_A$  within the model  $A_{\tilde{G}}(\varphi)$ , Eq. (4.4), and using the

same assumptions as in Fig. 3 [notably a maximally allowed value of  $\varphi_0$ , Eq. (4.5)]. We see in Fig. 4 that when  $m_A \gtrsim 1 m_\odot$ , we get very drastic modifications of the general relativistic prediction for  $\gamma$  (except in a small neighborhood of  $m_A \sim 1.3 m_\odot$  where  $K_A^A$  vanishes). In particular, when  $1.1 \leq m_A/m_\odot \leq 1.2$ ,  $K_A^A$  takes largish *negative* values which change the sign of the predicted  $\gamma^{\text{th}}$ . [The minimum value of  $K_A^A$  in Fig. 4 is reached for  $m_A = 1.13 m_\odot$  and equals  $K_A^{\text{Amin}} = -3.45$ , yielding  $\gamma_{\text{min}}^{\text{th}}(m_A, m_B) = -1.27 \gamma^{\text{GR}}$ .] We computed also  $K_A^A$  for smaller values of the external scalar field  $\varphi_0$  and found (as usual by now) that they cause a sharpening of the “resonance” bump in Fig. 4. For instance, we found that  $K_A^{\text{Amin}} = -6.68$  for  $\varphi_0 = \varphi_0^{\max}/10$ . Paradoxically, smaller values of the weak-field coupling  $\alpha_0$  predict larger values of the modification  $K_A^A$  to the timing parameter  $\gamma$ , though concentrated over a smaller range of mass values. This effect is even more spectacular for  $K_A^B$  when  $\bar{m}_B > \bar{m}_A \approx \bar{m}_{\text{cr}}$ : In that case, the effective coupling  $\alpha_B$  tends to a nonvanishing constant as  $\varphi_0 \rightarrow 0$ , while  $\partial \ln I_A / \partial \varphi_0$  blows up, so that  $|K_A^B|$  can take arbitrarily large values. For instance, one gets  $K_A^{\text{Bmin}} = -8.20$  for  $\varphi_0 = \varphi_0^{\max}$ , and  $K_A^{\text{Bmin}} = -23.82$  for  $\varphi_0 = \varphi_0^{\max}/10$  [yielding  $\gamma_{\text{min}}^{\text{th}}(m_A, m_B) \approx -23 \gamma^{\text{GR}}$ ]. Finally, varying the value of the curvature parameter  $\beta$  in the models (2.1) displaces the center of the bump in  $K_A^A$ , towards lower (higher) values when  $-\beta$  increases (decreases).

## V. APPLICATION TO BINARY-PULSAR EXPERIMENTS

We have now all the necessary tools in hand for exploring the impact of nonperturbative scalar effects on binary-pulsar experiments. In a future publication [11], we shall confront in a systematic manner the predictions of tensor-scalar gravitation theories with a more complete and updated set of binary-pulsar data. In the present work, we shall illustrate how binary-pulsar data give us very significant constraints on the strong-field regime of relativistic gravity by comparing published data<sup>11</sup> on PSR 1913+16, PSR 1534+12, and PSR 0655+64 with the predictions of tensor-scalar theories exhibiting the nonperturbative effects discussed above. In Ref. [11], we shall also take into account data on certain nearly circular binary systems which test the strong equivalence principle [22–24]. We do not consider them here because they are less constraining than the systems we study. [Indeed, the “Stark effect” is proportional to the product  $\alpha_0(\alpha_A - \alpha_B)$  and, therefore, is already significantly constrained by the solar-system limits on  $\alpha_0$ .]

The case of PSR 1913+16 is the richest in that it involves many different types of strong-field effects: (i) modifications of the first post-Keplerian orbital motion (observable through the periastron advance  $\dot{\omega}$ ), (ii) modification of gravitational radiation damping (observable through the orbital period decay  $\dot{P}_b$ ), and (iii) sensitivity of the pulsar inertia moment to

<sup>9</sup>Note in passing that the pulsar clock ticks neither the Einstein time nor the Jordan-Fierz one. Indeed, both  $I_A$  and  $\tilde{I}_A$  fluctuate because of their dependence on  $\varphi_A(t)$ .

<sup>10</sup>The general relativistic prediction  $\gamma^{\text{GR}}(m_A, m_B)$  is obtained from Eq. (4.9) by setting  $\alpha_A \alpha_B = 0$ ,  $G_{AB} = G$ , and  $K_A^B = 0$ .

<sup>11</sup>Note that the pulsar community now uses an updated notation in which these pulsars are called PSR B 1913+16, PSR B 1534+12, and PSR B 0655+64, respectively. Here, the label B (for Besselian) refers to the equatorial coordinate system based on the 1950 equinox [while the letter J (for Julian) refers to the 2000 equinox].

an external scalar field (observable through the timing parameter  $\gamma$ ). As we shall discuss below, the case of PSR 1534+12 very usefully complements that of 1913+16 in trading the  $\dot{P}_b$  measurement against a measurement of the shape parameter  $s$  of the gravitational delay. The scalar-field effects in  $\dot{\omega}$ ,  $\dot{P}_b$ , and  $s$  have been already worked out with sufficient accuracy in the literature [5,21,18], while the scalar-field effects in  $\gamma$  have been discussed above.

### A. PSR 1913+16 experiment

We recall that, at present, one can phenomenologically extract from the raw data of the binary pulsar PSR 1913+16 (following the methodology of [21]) *three* well-measured<sup>12</sup> observables  $\dot{\omega}^{\text{obs}}$ ,  $\gamma^{\text{obs}}$ , and  $\dot{P}_b^{\text{obs}}$ . Here  $\dot{\omega}^{\text{obs}}$  denotes the secular rate of advance of the periastron,  $\gamma^{\text{obs}}$  denotes the observed value of the timing parameter discussed above, and  $\dot{P}_b^{\text{obs}}$  denotes the secular change of the orbital period. The values we shall take for these observed parameters are [26]

$$\dot{\omega}^{\text{obs}} = 4.226\,621(11)^\circ \text{ yr}^{-1}, \quad (5.1a)$$

$$\gamma^{\text{obs}} = 4.295(2) \times 10^{-3} \text{ s}, \quad (5.1b)$$

$$\dot{P}_b^{\text{obs}} = -2.422(6) \times 10^{-12}, \quad (5.1c)$$

where figures in parentheses represent  $1\sigma$  uncertainties in the last quoted digits. We shall also need the Keplerian parameters

$$P_b = 27\,906.980\,780\,4(6) \text{ s}, \quad (5.2a)$$

$$e = 0.617\,130\,8(4). \quad (5.2b)$$

The important point (which is the basis of the parametrized post-Keplerian approach [21]) is that the observables (5.1) have been extracted from the raw pulsar data *without* assuming any specific gravitation theory (at least within the very wide class of boost-invariant theories). One can then use the three pieces of data (5.1) to constrain theories of gravitation. To do this one must compute, within the theory to be tested, what are the predictions it makes for  $\dot{\omega}$ ,  $\gamma$ , and  $\dot{P}_b$  as *functions* of the two (*a priori* unknown) masses  $m_A$ ,  $m_B$ . We have written in Eq. (4.9) above the theoretical prediction for the timing parameter,  $\gamma^{\text{th}}(m_A, m_B)$ , within tensor-scalar gravity models. The theoretical prediction for the periastron advance rate has been worked out in Refs. [18,21,5] and reads, with the notation of the present paper,

$$\begin{aligned} \dot{\omega}^{\text{th}}(m_A, m_B) = & \frac{3n}{1-e^2} \left( \frac{G_{AB}(m_A + m_B)n}{c^3} \right)^{2/3} \left[ \frac{1 - \frac{1}{3}\alpha_A\alpha_B}{1 + \alpha_A\alpha_B} \right. \\ & \left. - \frac{X_A\beta_B\alpha_A^2 + X_B\beta_A\alpha_B^2}{6(1 + \alpha_A\alpha_B)^2} \right]. \end{aligned} \quad (5.3)$$

The notation in Eq. (5.3) is the same as in Eq. (4.9). We recall that  $n \equiv 2\pi/P_b$ ,  $G_{AB} = G_*(1 + \alpha_A\alpha_B)$ , and

<sup>12</sup>Two more observables  $r^{\text{obs}}$  and  $s^{\text{obs}}$  are measured with low precision [25].

$X_A \equiv m_A/(m_A + m_B) \equiv 1 - X_B$ . Finally, the theoretical prediction for the (radiation-reaction driven) orbital period decay has been derived in Ref. [5] (with the full needed accuracy and for generic tensor-scalar theories). It is given as a sum of contributions:

$$\begin{aligned} \dot{P}_b^{\text{th}}(m_A, m_B) = & \dot{P}_\varphi^{\text{monopole}} + \dot{P}_\varphi^{\text{dipole}} + \dot{P}_\varphi^{\text{quadrupole}} + \dot{P}_{g^*}^{\text{quadrupole}} \\ & + (\dot{P}^{\text{gal}})^{\text{GR}} + \delta^{\text{th}}(\dot{P}^{\text{gal}}). \end{aligned} \quad (5.4)$$

The first three contributions correspond to energy lost to scalar waves (of monopolar, dipolar, and quadrupolar type, respectively). The fourth one corresponds to the energy lost to quadrupolar tensor waves (pure spin-2 field  $g_{\mu\nu}^*$ ). The explicit expressions of these four terms are given in Eqs. (6.52) of [5]. The fifth contribution is the value of the galactic contribution to the observable  $\dot{P}_b$  computed in [27] within the assumption (true in general relativity) that neutron stars fall like ordinary bodies in the gravitational field of the Galaxy. Finally, the sixth and last contribution is the modification of the galactic contribution due to the fact that, in tensor-scalar gravity, neutron stars fall differently from weakly self-gravitating bodies [Eq. (9.22) of [5]].

As usual, given a specific tensor-scalar theory, a value for the externally imposed asymptotic boundary condition  $\varphi_0$ , and a specific nuclear equation of state, the three equations  $\dot{\omega}^{\text{th}}(m_A, m_B) = \dot{\omega}^{\text{obs}}$ ,  $\gamma^{\text{th}}(m_A, m_B) = \gamma^{\text{obs}}$ , and  $\dot{P}_b^{\text{th}}(m_A, m_B) = \dot{P}_b^{\text{obs}}$  define three curves (in fact three *strips*) in the two-dimensional plane of the masses  $(m_A, m_B)$ . If the three strips meet in a small region, the considered tensor-scalar theory is consistent with the binary-pulsar data. If they do not meet, the considered theory is inconsistent with the pulsar observations.

Before presenting the results of such a confrontation for scalar models exhibiting nonperturbative effects, it is instruc-

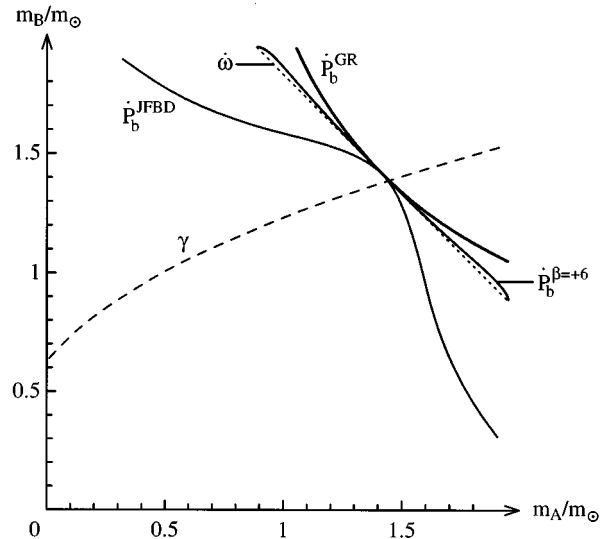


FIG. 5. The  $(\dot{\omega} - \gamma - \dot{P}_b)_{1913+16}$  test for general relativity (GR), the Jordan-Fierz-Brans-Dicke theory (JFBD), and the quadratic model  $A(\varphi) = \exp(+3\varphi^2)$  (corresponding to a positive-curvature parameter  $\beta = +6$ ). The widths of the three  $\dot{P}$  lines correspond to  $1\sigma$  standard deviations. The  $\dot{\omega}^{\text{th}} = \dot{\omega}^{\text{exp}}$  and  $\gamma^{\text{th}} = \gamma^{\text{exp}}$  lines are wider than  $1\sigma$  errors, and cannot be distinguished for the three theories.

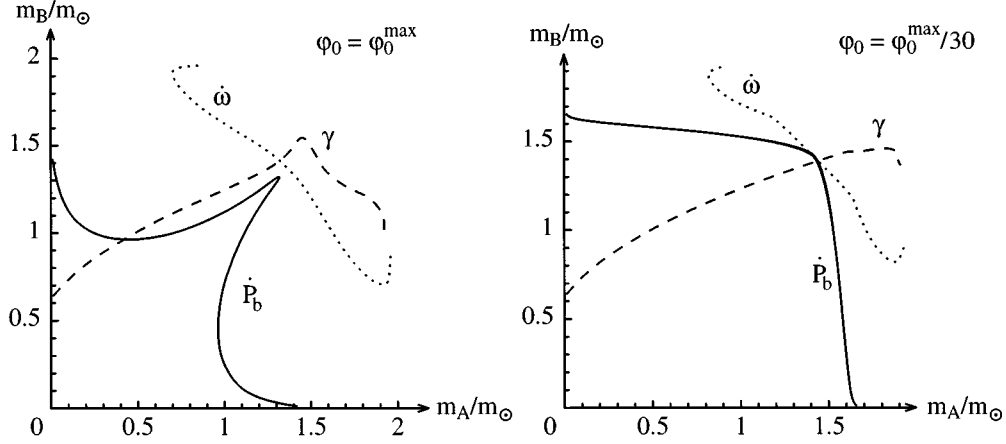


FIG. 6. The  $(\dot{\omega} - \gamma - \dot{P}_b)_{1913+16}$  test for the quadratic model  $A(\varphi) = \exp(\frac{1}{2}\beta\varphi^2)$  with  $\beta = -4.5$ , when  $\varphi_0$  takes the maximum value allowed by solar-system experiments (left panel), and a 30 times smaller value (right panel). In this figure and the following ones,  $1\sigma$  deviations are smaller than the width of the lines.

tive, for making a contrast, to discuss two other cases (besides the general relativistic one): (i) the case of the well-known Jordan-Fierz-Brans-Dicke (JFBD) theory [2–4] and (ii) the case of scalar-tensor models with *positive* curvature of the coupling function. The JFBD theory contains only one free parameter  $\alpha_0$  and is defined by the coupling function

$$A_{\text{JFBD}}(\varphi) = \exp(\alpha_0\varphi). \quad (5.5)$$

The scalar coupling strength in this theory is constant:  $\alpha(\varphi) \equiv \partial \ln A / \partial \varphi = \alpha_0$ . As a consequence (see Sec. II), it cannot exhibit nonperturbative effects. All deviations from general relativity, be they in weak-field or strong-field conditions, are proportional to  $\alpha_0^2$ , and are uniformly constrained by the solar-system limit (1.6). On the other hand, as discussed in [10], scalar-tensor models belonging to the quadratic class (2.1) with  $\beta > 0$  exhibit nonperturbative effects of a deamplification type: Deviations from general relativity are exponentially suppressed by strong-field effects, i.e., are proportional to  $\alpha_0^2 \exp(-3\beta s_A)$ , where  $s_A \sim 0.2$  is a measure of the strength of the self-gravity of the considered neutron star.

As one of the aims of the present work is to delineate the cases where binary-pulsar data give more stringent constraints than solar system data on tensor-scalar theories, we shall draw the figures below (except when otherwise indicated) under the assumption that the externally imposed  $\varphi_0$  always takes the maximum value allowed by solar-system tests. As said above, the corresponding value of  $\varphi_0$  depends on the theory considered and is determined from combining the two inequalities (1.6) and (4.6). Figure 5 exhibits the curves defined by the observables  $\dot{\omega}$ ,  $\gamma$ , and  $\dot{P}_b$  in PSR 1913+16 when interpreted in the framework of three different theories: general relativity, Jordan-Fierz-Brans-Dicke, and the quadratic model (2.1) with  $\beta = +6$ . This plot illustrates the fact that binary pulsars involving nearly equal

mass<sup>13</sup> neutron stars do not constrain more severely than solar-system data theories with logarithmic coupling functions  $\ln A(\varphi)$  which are either linear (or nearly linear) in  $\varphi$  [28] or have a *positive* curvature [i.e., convex functions  $\ln A(\varphi)$ ]. Note that the  $\dot{P}_b$  curve of a quadratic model with positive curvature lies between the general relativistic and the JFBD ones. The fact that in Fig. 5 the  $\dot{P}_b^{\beta=+6}$  curve almost overlaps with the  $\dot{\omega}$  curve is a numerical coincidence caused by our choices for  $\beta$  and  $\varphi_0$ .

By contrast, tensor-scalar theories involving sufficiently *concave* functions  $\ln A(\varphi)$ , i.e., models (2.1) with  $\beta$  sufficiently negative, show a very different behavior when confronted to pulsar data. This is illustrated in the remaining figures. The left panel of Fig. 6 shows that although the quadratic model  $A_{-4.5}(\varphi)$  [i.e.,  $\beta = -4.5$  in Eq. (2.1)] can pass all present solar-system tests, it fails the  $(\dot{\omega} - \gamma - \dot{P}_b)_{1913+16}$  test. For such a model, pulsar observations constrain more strongly the theory than weak-field tests. This is further illustrated in the right panel of this figure, which shows that one needs a smaller value of  $\varphi_0$ , i.e., a smaller value of  $\alpha_0 = \beta\varphi_0$ , than the maximal one allowed by solar data. We did not make an exhaustive numerical search but it seems that a value  $\alpha_0^{\text{PSR}} \sim \frac{1}{30} \alpha_0^{\text{max}}$  is the correct order of magnitude that pulsar data can tolerate. Note that, in terms of the basic Eddington parameters  $\bar{\gamma} \equiv \gamma_{\text{Edd}} - 1 \approx -2\alpha_0^2$ ,  $\bar{\beta} \equiv \beta_{\text{Edd}} - 1 \approx \frac{1}{2}\beta_0\alpha_0^2$ , this means that binary-pulsar data are 1000 times more constraining than solar-system tests, constraining  $\bar{\gamma}$  and  $\bar{\beta}$  [for the considered model  $A_{-4.5}(\varphi)$ ] below the  $10^{-6}$  level.

In the above case ( $\beta = -4.5$ ), the fact that the maximal weak-field-allowed value of  $\varphi_0$  was forbidden, while a 30

<sup>13</sup>As emphasized by Eardley [17], the situation is different for unequal mass systems thanks to the presence of scalar dipole radiation  $\propto (\alpha_A - \alpha_B)^2$ . This shows up in Fig. 5 as a strong distortion of the  $\dot{P}_b$  curve away from the diagonal  $m_A = m_B$ . See below our study of the unequal mass system PSR 0655+64.

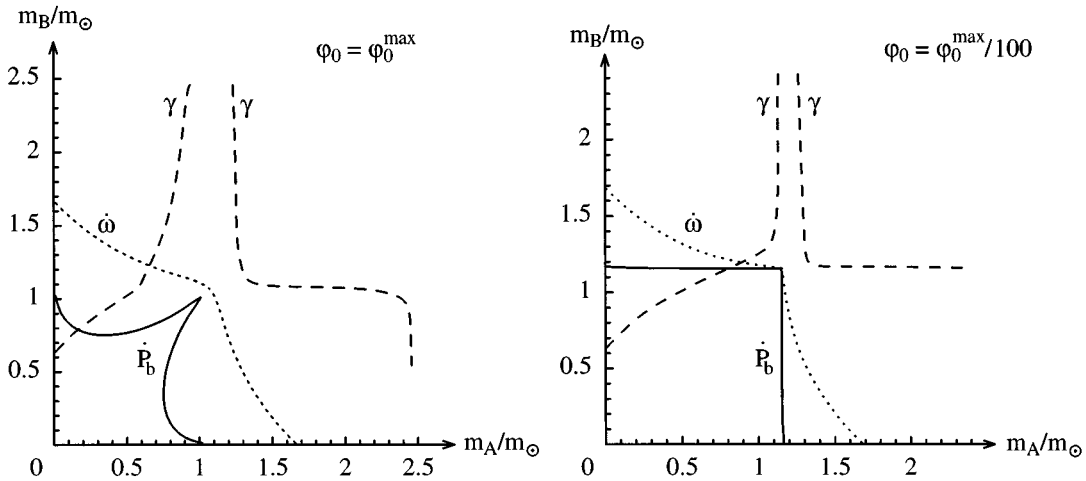


FIG. 7. The  $(\dot{\omega} - \gamma - \dot{P}_b)_{1913+16}$  test for the quadratic model  $A(\varphi) = \exp(-3\varphi^2)$  (i.e.,  $\beta = -6$ ), when  $\varphi_0$  takes the maximum value allowed by solar-system experiments (left panel), and a 100 times smaller value (right panel).

times smaller one was allowed, was due to the presence of significant nonperturbative scalar effects for  $\varphi_0 = \varphi_{0\text{solar}}^{\text{max}}$  which tended to zero when  $\varphi_0 \rightarrow 0$ . This smooth disappearance of nonperturbative effects when  $\varphi_0 \rightarrow 0$  was connected to the fact that the critical value of the mass  $\bar{m}_{\text{cr}}$  (above which spontaneous scalarization occurs in zero-external-field conditions) is slightly larger than the actual mass of the stars [ $\bar{m}_{\text{cr}}(\beta = -4.5) \approx 1.84m_\odot$  while  $\bar{m}_A^{\text{best fit}} \approx \bar{m}_B^{\text{best fit}} \approx 1.5m_\odot$ ].

A quite different situation arises for values of  $-\beta$  large enough to make  $\bar{m}_{\text{cr}}$  smaller than the masses of the stars. This case is illustrated in Fig. 7 where one confronts pulsar data with the model  $A_{\bar{\varphi}}$ , Eq. (4.4). [In this model  $\bar{m}_{\text{cr}}(\beta = -6) \approx 1.24m_\odot$ .] This figure shows that the model  $A_{\bar{\varphi}}$  fails very badly the  $(\dot{\omega} - \gamma - \dot{P}_b)_{1913+16}$  test, while it can pass all present solar-system tests. Especially remarkable is the wild behavior of the  $\gamma$  curve, which is due to the large values of the  $K_A^B$  deviation discussed in the previous section (see Fig. 4 there). In that case, this disagreement between theory and experiment is *not* alleviated by considering smaller values of  $\varphi_0$ , as illustrated on the right panel of Fig. 7. From our numerical results, we find that the  $(\dot{\omega} - \gamma - \dot{P}_b)_{1913+16}$  test can be passed, if at all, only for extremely fine-tuned values of the masses in close neighborhoods of the critical values  $\bar{m}_A \approx \bar{m}_B \approx \bar{m}_{\text{cr}}$ . Barring any fine-tuned coincidence, we conclude that the tensor-scalar theory defined by  $A_{\bar{\varphi}}(\varphi)$  is incompatible with pulsar data *whatever be the value of  $\varphi_0$* , even infinitely smaller than  $\varphi_{0\text{solar}}^{\text{max}}$ . This remarkable conclusion proves explicitly that pulsar data are *qualitatively* different from solar-system data in their probing power of relativistic gravity. The theory defined by  $A_{\bar{\varphi}}(\varphi)$  could always be made compatible with solar-system tests of any precision,<sup>14</sup> while it is already falsified by existing pulsar observations. As the critical mass  $\bar{m}_{\text{cr}}$  decreases when  $-\beta$  increases, the confrontation between theory and pulsar experiments can only get worse when  $-\beta > 6$ . Furthermore, our (partial) numerical exploration of

the range  $-6 < \beta < -4.5$  shows that values of  $\beta$  smaller than  $-5$  are already excluded. [This will be illustrated by an exclusion plot discussed below.] We conclude that present PSR 1913+16 data already exclude all “quadratic” models (2.1) with  $\beta < -5$ .

### B. PSR 1534+12 experiment

One conceivable deficiency in the above argument is the possible presence of a cosmological variation of  $\varphi_0$ . Indeed, a nonzero value of  $\dot{\varphi}_0 \equiv d\varphi_0/dt_0$  entails a secular variation of the strength of scalar gravity and produces an additional contribution in  $\dot{P}_b^{\text{th}}$ . From the observed  $\dot{P}_b^{\text{obs}}$ , one cannot decorrelate  $\dot{\varphi}_0$  effects from scalar modifications to radiation damping. One way to decorrelate  $\dot{\varphi}_0$  effects is to consider pulsar experiments which are insensitive to  $\dot{\varphi}_0$ . Such is the case of the measurements of the three observables  $\dot{\omega}^{\text{obs}}$ ,  $\gamma^{\text{obs}}$ , and  $s^{\text{obs}}$  in PSR 1534+12. Here  $s^{\text{obs}}$  denotes a phenomenological parameter measuring the shape of the gravitational time delay [20,21]. The values we shall take for these three<sup>15</sup> observable parameters are [23]

$$\dot{\omega}^{\text{obs}} = 1.755\,73(4)^\circ \text{ yr}^{-1}, \quad (5.6a)$$

$$\gamma^{\text{obs}} = 2.081(16) \times 10^{-3}, \quad (5.6b)$$

$$s^{\text{obs}} = 0.981(8). \quad (5.6c)$$

We shall also need the Keplerian observables

$$P_b = 36\,351.702\,67(2) \text{ s}, \quad (5.7a)$$

$$e = 0.273\,677\,1(4), \quad (5.7b)$$

$$x = 3.729\,458(2) \text{ s}. \quad (5.7c)$$

The theoretical predictions for  $\dot{\omega}^{\text{th}}$  and  $\gamma^{\text{th}}$  have been written above. That for  $s^{\text{th}}$  reads [21]

<sup>14</sup>For argument’s sake we assume here that general relativity is the correct theory of gravity.

<sup>15</sup>We do not consider here the other observables  $r^{\text{obs}}$  and  $\dot{P}_b^{\text{obs}}$  which are measured with low fractional precision.



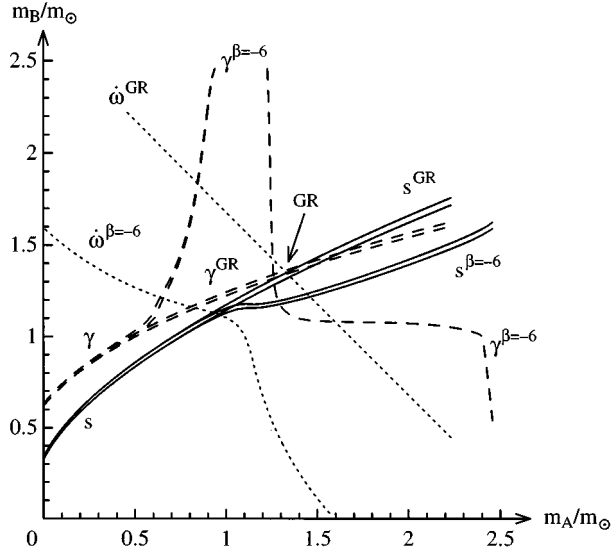


FIG. 8. The  $(\dot{\omega} - \gamma - s)_{1534+12}$  test for general relativity (GR) and for the quadratic model  $A(\varphi) = \exp(-3\varphi^2)$  (i.e.,  $\beta = -6$ ) when  $\varphi_0$  takes the maximum value allowed by solar-system experiments. The widths of the strips correspond to  $1\sigma$  standard deviations. The arrow indicates the intersection of the three strips in general relativity. In the model  $\beta = -6$ , the three strips do not intersect.

$$s = \frac{nx}{X_B} [G_{AB}(m_A + m_B)n/c^3]^{-1/3}, \quad (5.8)$$

where we have used the same notation as in Eqs. (4.9) and (5.3) above, and where  $x = a_1 s/c$  is the projection of the semimajor axis ( $a_1$ ) of the pulsar orbit on the line of sight (in light-seconds).

We have plotted the three curves defined by this  $(\dot{\omega} - \gamma - s)_{1534+12}$  test for various values of  $\beta$  and  $\varphi_0$ . For instance, we exhibit the case  $\beta = -6$ ,  $\varphi_0 = \varphi_{0\text{solar}}^{\text{max}}$  in Fig. 8 (together with the case of general relativity). From our (partial) numerical study, we conclude that the quadratic models  $A_\beta$  fail the  $(\dot{\omega} - \gamma - s)_{1534+12}$  test when  $\beta < -5.5$ . The corresponding exclusion plot is very similar to that defined by PSR 1913+16 (see below).

### C. PSR 0655+64 experiment

The binary pulsar PSR 0655+64 is composed of a neutron star of mass  $\approx 1.4m_\odot$  and a white dwarf companion of mass  $\approx 0.8m_\odot$ . They move around each other on a nearly circular orbit in a period of about 1 day. In tensor-scalar gravity, such a dissymmetrical system is a powerful emitter of dipolar scalar waves, especially in the presence of nonperturbative scalar effects. The theoretical prediction [5] for the corresponding orbital period decay is dominated by the  $O(v^3/c^3)$  dipole contribution in Eq. (5.4) above:

$$\dot{P}_b^{\text{th}}(m_A, m_B) \approx \dot{P}_\varphi^{\text{dipole}} = - \frac{2\pi G_* m_A m_B n}{(m_A + m_B) c^3} \frac{1 + e^2/2}{(1 - e^2)^{5/2}} \times (\alpha_A - \alpha_B)^2 + O\left(\frac{v^5}{c^5}\right). \quad (5.9)$$

The fact that the observed value of  $\dot{P}_b$  in PSR 0655+64 is very small (and, in fact, consistent with zero) constrains very much the magnitude of the effective coupling strength  $\alpha_A$ , and therefore the possibility of nonperturbative effects. The experimental data we need for our analysis are taken from Ref. [23]:

$$P_b = 88\,877.061\,94(4) \text{ s}, \quad (5.10a)$$

$$e < 3 \times 10^{-5}, \quad (5.10b)$$

$$x \equiv (a_1 \sin i)/c = 4.125\,60(2) \text{ s}, \quad (5.10c)$$

$$\dot{P}_b = (1 \pm 4) \times 10^{-13}. \quad (5.10d)$$

The masses of the pulsar and its companion are not known independently. From the observed mass function, the *a priori* statistics of the inclination angle  $i$ , and the observed small statistical spread of neutron star masses around  $1.35m_\odot$ , one can deduce a range of probable values for the pair  $(m_A, m_B)$ : Essentially, one is limited to a subregion of the rectangle  $m_A = (1.35 \pm 0.05)m_\odot$ ,  $m_B = (0.8 \pm 0.1)m_\odot$  in the mass plane<sup>16</sup> [23]. In our calculations, we will choose the mass pair which gives the most conservative bounds on tensor-scalar gravity, namely,  $m_A = 1.30m_\odot$ ,  $m_B = 0.7m_\odot$ .

Finally, using the fact that the self-gravity of the white dwarf companion is negligible compared to that of the pulsar (so that  $\alpha_B \approx \alpha_0$ ), we get from Eqs. (5.9) and (5.10) the  $1\sigma$  level constraint

$$[\alpha_A(m_A) - \alpha_0]^2 < 3 \times 10^{-4}. \quad (5.11)$$

### D. Exclusion plots within a generic two-dimensional plane of tensor-scalar theories

It is instructive to contrast the pulsar constraints on tensor-scalar gravity with the constraints obtained from solar-system experiments. We can use the class of quadratic models (2.1) as a generic description of the shape of the coupling function around the current cosmological value of  $\varphi$ . In other words, we can parametrize an interesting class of tensor-scalar models by two parameters:<sup>17</sup> say,  $\alpha_0 \equiv \alpha(\varphi_0)$  and  $\beta_0 \equiv \partial\alpha(\varphi_0)/\partial\varphi_0$ . (In quadratic models,  $\alpha_0 = \beta\varphi_0$ , and  $\beta_0 = \beta$  is field independent.) We can then interpret all experimental data (solar-system and pulsar ones) as constraints in the two-dimensional theory plane  $(\alpha_0, \beta_0)$ . For instance, neglecting the correlations in the measurements of the two Eddington parameters  $\gamma_{\text{Edd}}$  and  $\beta_{\text{Edd}}$ , solar-system data rule out the regions of the  $(\alpha_0, \beta_0)$  plane where the inequalities  $|\gamma_{\text{Edd}} - 1| < 2 \times 10^{-3}$  (i.e.,  $\alpha_0^2 < 10^{-3}$ ) [8] and  $|\beta_{\text{Edd}} - 1| < 6 \times 10^{-4}$  (i.e.,  $|\beta_0| \alpha_0^2 < 1.2 \times 10^{-3}$ ) [19] are not

<sup>16</sup>We use here the fact that the scalar modifications to the link between the observed mass function  $n^2(a_1 \sin i)^3$  and the Einstein masses  $m_A, m_B$  due to the factor  $G_{AB}/G = 1 + \alpha_A \alpha_B$  are small because  $\alpha_B \approx \alpha_0$  for the white dwarf companion.

<sup>17</sup>This two-parameter class of models is representative of the large class of coupling functions  $A(\varphi)$  which admit a local minimum and contain no large dimensionless parameters [i.e., we assume that higher derivatives  $\beta'_0 \equiv \partial\beta(\varphi_0)/\partial\varphi_0$ ,  $\beta''_0 \equiv \partial^2\beta(\varphi_0)/\partial\varphi_0^2$  are of order unity].

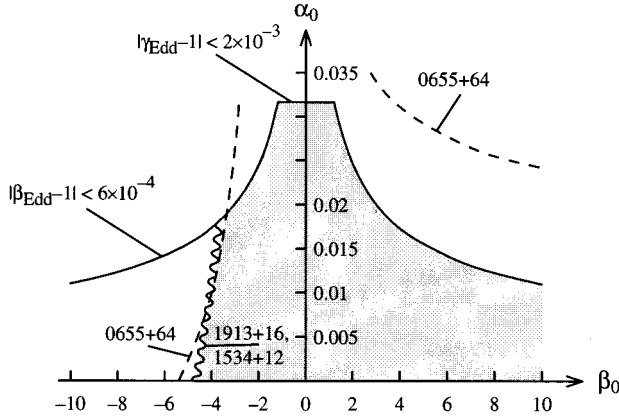


FIG. 9. Regions of the  $(\alpha_0, \beta_0)$  plane allowed by solar-system experiments and three binary-pulsar experiments. In view of the reflection symmetry  $\alpha_0 \rightarrow -\alpha_0$ , we plot only the upper half plane. The region allowed by solar-system tests is below the solid line. The PSR 0655+64 test constrains the values of  $\alpha_0$  and  $\beta_0$  to be between the two dashed lines. The region allowed by the PSR 1913+16 and PSR 1534+12 tests lies to the right of the (approximate) wavy line. The region simultaneously allowed by all the tests is shaded.

satisfied. The corresponding exclusion plot is represented in Fig. 9. In the same plot, we can represent the constraints brought by pulsar data on tensor-scalar models. The PSR 1913+16 and PSR 1534+12 data give constraints which are numerically similar. Taken together, they exclude the region to the left of the wavy line indicated on Fig. 9. This line is approximate and was obtained by interpolating between a few values of  $\alpha_0$  and  $\beta_0$ . We leave to future work a detailed study of the precise region of the  $(\alpha_0, \beta_0)$  plane excluded by these pulsar data.

As for the PSR 0655+64 data, they define through Eq. (5.11) (with the conservative value  $m_A = 1.30m_\odot$ ) another limit on tensor-scalar models. We have numerically computed the region of the  $(\alpha_0, \beta_0)$  plane defined by the inequality (5.11). The corresponding allowed region is contained within the two dashed lines labeled 0655+64 on Fig. 9. The region simultaneously allowed by all the tests is shaded.

To prevent any confusion, let us note that the limit on the 2PN parameter  $\zeta \equiv \beta_0^2 \alpha_0^2 / (1 + \alpha_0^2)^3$ , obtained in a recent simplified *analytical* study of combined pulsar data [7], is valid only for  $|\beta| \leq 1$ . Indeed, the approximate treatment of [7] assumed the absence of any nonperturbative effect, i.e., an absolute value of  $\beta_0$  appreciably smaller than 4. The PSR 0655+64 constraint studied here should merge with the limit  $\beta_0^2 \alpha_0^2 < 4 \times 10^{-3}$  derived in [7] when  $|\beta_0| \leq 1$ . [We use here the inequality (5.24c) of Ref. [7] together with the theoretical constraint that  $\beta_0^2 \alpha_0^2$  be positive.] This merging occurs anyway in a region which is already excluded by solar-system data.

## VI. CONCLUSIONS

Before summarizing the main results of the present work, we wish to indicate briefly the frameworks within which our findings might be physically relevant. First, let us note that (barring any unnatural fine tuning) they are not relevant in

the case of a strictly massless scalar field  $\varphi$ , or at least when its mass  $m_\varphi \ll \hbar H_0 / c^2 \sim h_{100} \times 2.13 \times 10^{-33}$  eV, where  $H_0 = h_{100} \times 100$  km s<sup>-1</sup>/Mpc denotes Hubble's constant. Indeed, in such a case it was found, both in traditional equivalence-principle-respecting tensor-scalar theories [29] and in string-inspired models with a massless dilaton or modulus [6], that the cosmological evolution naturally drives the vacuum expectation value of  $\varphi$  toward *minima* of  $\ln A(\varphi)$ . As the latter vacuum expectation value coincides (modulo small *fractional* corrections due to spatial fluctuations of the gravitational potential [7]) with our externally imposed  $\varphi_0$ , a natural prediction of these massless models is that  $\alpha_0 = \partial \ln A(\varphi_0) / \partial \varphi_0$  is small and that  $\beta_0 = \partial^2 \ln A(\varphi_0) / \partial \varphi_0^2$  is *positive*. The former result concerning  $\alpha_0$  is in agreement with observational data, but the latter one concerning  $\beta_0$  gives the wrong sign for spontaneous scalarization effects.<sup>18</sup>

On the other hand, our results are relevant to the wide class of models comprising scalar fields of range<sup>19</sup>  $10^6$  km  $\leq \lambda = \hbar / m_\varphi c \leq c H_0^{-1}$ . Assuming that the endemic ‘‘Polonyi problem’’ [too much energy stored in the cosmological oscillations of  $\varphi_0(t)$ ] [30] of such models is somehow solved [31] or fine-tuned to provide  $\Omega = \rho_{\text{tot}} / \rho_{\text{cr}} = 1$  [32], the condition for these models to be naturally compatible with solar-system constraints is simply that the location  $\varphi_0$  of the minimum of the  $\varphi$  potential,  $V(\varphi) = (c^4 / 8\pi G_*) m_\varphi^2 (\varphi - \varphi_0)^2$ , coincide (or nearly coincide) with an *extremum* of the coupling function  $A(\varphi)$ . Such a coincidence would, for instance, naturally follow from a discrete symmetry about  $\varphi_0$ , say, a reflection symmetry  $(\varphi - \varphi_0) \rightarrow -(\varphi - \varphi_0)$  [6]. Under such a condition, the present value of the weak-field scalar coupling  $\alpha_0 = \partial \ln A(\varphi_0) / \partial \varphi_0$  would be naturally extremely small, and the sign of the curvature  $\beta_0 = \partial^2 \ln A(\varphi_0) / \partial \varphi_0^2$  could be expected to be negative with *a priori* 50% probability.

As a simple example of such models, we can consider a finite-range scalar field coupled only to the gravitational sector through a multiplicative coupling to the scalar curvature, say,

$$S = \frac{c^4}{16\pi G_*} \int \frac{d^4x}{c} \tilde{g}^{1/2} (-Z(\Phi) \tilde{g}^{\mu\nu} \partial_\mu \Phi \partial_\nu \Phi - U(\Phi) + F(\Phi) \tilde{R}) + S_m[\psi_m; \tilde{g}_{\mu\nu}], \quad (6.1)$$

where we have introduced the possibility of an arbitrary field-dependent normalization of the kinetic term of  $\Phi$ . One transforms Eq. (6.1) into our canonical form (1.1) [completed by a  $\varphi$ -potential term  $V(\varphi) = (c^4 / 16\pi G_*) F^{-2}(\Phi) U(\Phi)$ ] by defining

<sup>18</sup>Note, however, that a coupling function of the type  $\ln A(\varphi) = +\epsilon^2 \varphi^2 - \lambda^2 \varphi^4$ , with a sufficiently small  $\epsilon$  and a sufficiently large  $\lambda$ , would reconcile a (very localized) minimum at  $\varphi = 0$  with a mainly concave coupling function leading to nonperturbative effects. We do not wish to consider here such fine-tuned cases.

<sup>19</sup>The lower bound comes from the requirement that  $\varphi$  be effectively massless on the scale of a typical binary pulsar. If it is violated, one must correct our formulas by Yukawa exponential factors.

$$g_{\mu\nu}^* = F(\Phi) \tilde{g}_{\mu\nu}, \quad (6.2a)$$

$$\varphi = \int d\Phi \left[ \frac{3}{4} \frac{F'^2(\Phi)}{F^2(\Phi)} + \frac{1}{2} \frac{Z(\Phi)}{F(\Phi)} \right]^{1/2}. \quad (6.2b)$$

This corresponds to a coupling function

$$A(\varphi) = F^{-1/2}(\Phi). \quad (6.3)$$

The simplest example of such models is a massive scalar having a nonminimal dimensionless coupling to curvature:

$$S = \frac{c^4}{16\pi G_*} \int \frac{d^4x}{c} \tilde{g}^{1/2} (-\tilde{g}^{\mu\nu} \partial_\mu \Phi \partial_\nu \Phi - m_\Phi^2 \Phi^2 + \xi \tilde{R} \Phi^2 + \tilde{R}) + S_m[\psi_m; \tilde{g}_{\mu\nu}]. \quad (6.4)$$

This corresponds to  $Z(\Phi)=1$ ,  $U(\Phi)=m_\Phi^2 \Phi^2$ , and  $F(\Phi)=1+\xi\Phi^2$ . In that case, one can integrate Eq. (6.2b) explicitly. Assuming for instance that  $\xi(1+6\xi)>0$  and introducing the notation  $\chi \equiv \sqrt{\xi(1+6\xi)}$ , one gets

$$2\sqrt{2}(\varphi - \varphi_0) = \frac{\chi}{\xi} \ln[1 + 2\chi\Phi(\sqrt{1+\chi^2\Phi^2} + \chi\Phi)] + \sqrt{6} \ln \left[ 1 - 2\sqrt{6}\xi\Phi \frac{\sqrt{1+\chi^2\Phi^2} - \sqrt{6}\xi\Phi}{1+\xi\Phi^2} \right]. \quad (6.5)$$

Note that  $(\varphi - \varphi_0) = \Phi/\sqrt{2} + O(\Phi^3)$  when  $\Phi \rightarrow 0$ . From Eqs. (6.2) and (6.3), one gets easily the parametric representations

$$A(\varphi) = (1 + \xi\Phi^2)^{-1/2}, \quad (6.6a)$$

$$\alpha(\varphi) = \frac{\partial \ln A(\varphi)}{\partial \varphi} = -\sqrt{2}\xi\Phi[1 + \xi(1+6\xi)\Phi^2]^{-1/2}, \quad (6.6b)$$

$$\beta(\varphi) = \frac{\partial^2 \ln A(\varphi)}{\partial \varphi^2} = -2\xi(1 + \xi\Phi^2)[1 + \xi(1+6\xi)\Phi^2]^{-2}. \quad (6.6c)$$

In particular the value of the curvature parameter around  $\varphi_0$  reads

$$\beta_0 = \beta(\varphi_0) = \left. \frac{\partial^2 \ln A(\varphi)}{\partial \varphi^2} \right|_{\Phi=0} = -2\xi. \quad (6.7)$$

Therefore, positive values of  $\xi$  [which, in the formulation (6.4), seem preferred because unable to cause a change of sign of the coefficient  $(1 + \xi\Phi^2)$  of the kinetic term for  $\tilde{g}_{\mu\nu}$ ] correspond to the “interesting” case where spontaneous scalarization effects can occur.<sup>20</sup>

<sup>20</sup>In our conventions, the so-called “conformal coupling” corresponds to  $\xi = -\frac{1}{6}$  and to a coupling function  $A(\varphi) = \cosh(\varphi/\sqrt{3})$ . Note, however, that only the action  $S_{\text{conf}} \equiv \int d^4x \tilde{g}^{1/2} [-\tilde{g}^{\mu\nu} \partial_\mu \Phi \partial_\nu \Phi - \frac{1}{2} \tilde{R} \Phi^2]$  (without bare Einstein term) exhibits a conformal invariance [33]. The action  $S_{\text{conf}}$  involves a spin-2 but no spin-0 excitation.

Let us now summarize the main results of the present work.

We have clarified the physical meaning of the nonperturbative strong-gravitational-field effects discovered in [10] by interpreting them, by analogy with ferromagnetism, as a phenomenon of “spontaneous scalarization.” Negative values of the curvature parameter  $\beta_0$  (like negative values of the coupling between magnetic moments  $H_{ij} = g \mu_i \mu_j$ ) favor the spontaneous creation of a scalar field when considered in the context of gravitationally compact objects (neutron stars). The critical baryonic mass for the spontaneous scalarization transition is  $\lesssim 1.5m_\odot$  when  $\beta_0 \lesssim -5$ . See Table I and Fig. 2 for precise values. The presence of some externally imposed scalar field background  $\varphi_0$  with  $\alpha_0 = \partial \ln A(\varphi_0)/\partial \varphi_0 \neq 0$  smoothes the scalarization transition (analogously to the presence of an external magnetic field for the ferromagnetic transition).

The development (through the previous mechanism) of strong scalar fields in neutron stars leads to very significant deviations from general relativity. These deviations are measured by some gravitational form factors  $\alpha_A, \beta_A, K_A^B$  which enter the effects observable in binary-pulsar experiments. In our previous work [10] we focused on the effective scalar coupling constant  $\alpha_A$ . Here, we gave results for  $\beta_A = \partial \alpha_A / \partial \varphi_0$  (see also [34]) and for  $K_A^B = -\alpha_B \partial \ln I_A / \partial \varphi_0$  which enters the parametrized post-Keplerian timing parameter  $\gamma$ . To compute  $K_A^B$ , we generalized to a tensor-scalar context the work of Hartle [13] on the general relativistic inertia moments  $I_A$  of slowly rotating neutron stars. We found that  $K_A^B$  could cause very drastic deviations from general relativity in tensor-scalar theories containing no large dimensionless parameters. This is achieved without fine-tuning and in theories having only positive-energy excitations.

We presented a preliminary investigation of the confrontation between scalar models exhibiting nonperturbative effects and actual binary-pulsar experiments. We contrasted the probing power of pulsar experiments to that of solar-system ones by working in the two-dimensional  $[\alpha_0 \equiv \partial \ln A(\varphi_0)/\partial \varphi_0, \beta_0 \equiv \partial^2 \ln A(\varphi_0)/\partial \varphi_0^2]$  plane describing a generic class of tensor-scalar models. Using published data on PSR’s 1913+16, 1534+12, and 0655+64 (and a specific nuclear equation of state), we found that binary-pulsar experiments exclude a large domain of theories compatible with solar-system experiments (see the exclusion plot, Fig. 9). In particular, they constrain  $\beta_0$  (independently of  $\alpha_0$ ) to

$$\beta_0 > -5. \quad (6.8)$$

Interestingly, this bound can be expressed in terms of the well-known weak-field Eddington parameters

$$\frac{\beta_{\text{Edd}} - 1}{\gamma_{\text{Edd}} - 1} < 1.3. \quad (6.9)$$

The singular (0/0) nature of the ratio on the left-hand side vividly expresses the fact that such a conclusion could never be obtained in weak-field experiments (at least until they find a significant deviation from general relativity). It must be kept in mind that the inequality (6.9) is one sided only, and that  $\beta_{\text{Edd}} - 1$  and  $\gamma_{\text{Edd}} - 1$  must be taken with their signs.

Let us note that, on the whole, the fact that pulsar data tend to exclude sufficiently negative values of  $\beta_0$  is nicely compatible with the expectation from cosmological attractor scenarios [29,6] that  $\varphi_0$  be dynamically driven toward a *minimum* of  $\ln A(\varphi)$ . Though our results have been derived by assuming a particularly simple coupling function between the scalar field and matter (“quadratic model”:  $\ln A(\varphi) = \frac{1}{2}\beta_0\varphi^2$ ), we think they hold in general classes of coupling functions containing no small or large dimensionless parameters. In a future publication [11], we shall present a more systematic confrontation between tensor-scalar theories and binary-pulsar experiments.

Before ending this paper, we would like to stress some of the limitations of our treatment that we intend to overcome in future work: (i) We considered here only one specific equation of state, modeled as a simple polytrope; a more complete study should consider a selection of realistic equations of state. (ii) In the present paper, we did not consider the effect of a cosmological variation of  $\varphi_0$ . We are aware that a nonzero  $\dot{\varphi}_0$  of order the Hubble parameter could significantly modify the interpretation of some of the pulsar tests discussed above. However, as one disposes of several independent pulsar tests, some of which do not involve  $\varphi_0$ -sensitive observables [such as the  $(\dot{\omega} - \gamma - s)_{1534+12}$  test considered above and several “Stark” tests [22–24]], we

think that a combined discussion of all pulsar tests will lead to limits on  $\alpha_0$  and  $\beta_0$  similar to the ones we have obtained here, and, in addition, to significant limits on  $\dot{\varphi}_0$ .

Finally, let us note that the strong scalar field effects discussed in [10] and the present paper could have a very significant impact on several aspects of the theory of gravitational radiation from compact objects [in addition to the ones taken into account in Sec. 6.2 of [5] and Eq. (5.4) above]. Of particular interest would be (i) the opening of a new, significant energy-loss channel in (spherically symmetric) gravitational collapse and neutron-star binary coalescences, and (ii) important modifications in the conditions for the onset of radiative instabilities in fast-rotating neutron stars (Chandrasekhar-Friedman-Schutz instability) [35]. Both issues are particularly worthy of further study.

### ACKNOWLEDGMENTS

We thank J.H. Taylor and S.E. Thorsett for informative discussions. The work of T. Damour at the Institute for Advanced Study was supported by the Monell Foundation. The work of G. Esposito-Farèse at Brandeis University was supported by Centre National de la Recherche Scientifique; partial support by NSF Grant No. PHY-9315811 is also gratefully acknowledged.

- 
- [1] T. Kaluza, Sitz. Preuss. Akad. Wiss. **1921**, 966 (1921).
  - [2] P. Jordan, Nature (London) **164**, 637 (1949); *Schwerkraft und Weltall* (Vieweg, Braunschweig, 1955); Z. Phys. **157**, 112 (1959).
  - [3] M. Fierz, Helv. Phys. Acta **29**, 128 (1956).
  - [4] C. Brans and R.H. Dicke, Phys. Rev. **124**, 925 (1961).
  - [5] T. Damour and G. Esposito-Farèse, Class. Quantum Grav. **9**, 2093 (1992).
  - [6] T. Damour and A.M. Polyakov, Nucl. Phys. **B423**, 532 (1994); Gen. Relativ. Gravit. **26**, 1171 (1994).
  - [7] T. Damour and G. Esposito-Farèse, Phys. Rev. D **53**, 5541 (1996).
  - [8] R.D. Reasenberg *et al.*, Astrophys. J. **234**, L219 (1979); D.S. Robertson, W.E. Carter, and W.H. Dillinger, Nature (London) **349**, 768 (1991); D.E. Lebach *et al.*, Phys. Rev. Lett. **75**, 1439 (1995). When interpreted in terms of our necessarily negative  $\gamma_{\text{Edd}} - 1 \approx -2\alpha^2$ , all the above references give essentially the same limit  $2\alpha^2 < 2 \times 10^{-3}$  (estimated standard error).
  - [9] T. Damour and D. Vokrouhlický, Phys. Rev. D **53**, 4177 (1996).
  - [10] T. Damour and G. Esposito-Farèse, Phys. Rev. Lett. **70**, 2220 (1993).
  - [11] T. Damour, G. Esposito-Farèse, and J.H. Taylor (in preparation).
  - [12] J. Diaz-Alonso and J.M. Ibañez-Cabanell, Astrophys. J. **291**, 308 (1985).
  - [13] J.B. Hartle, Astrophys. J. **150**, 1005 (1967).
  - [14] B. Carter, in *Gravitation in Astrophysics (Cargèse 1986)*, Proceedings of the NATO Advanced Study Institute, Cargèse, France, edited by B. Carter and J.B. Hartle, NATO ASI Series B: Physics Vol. 156 (Plenum, New York, 1987), p. 63.
  - [15] K. Just, Z. Naturforsch. **14**, 751 (1959).
  - [16] R. Coquereaux and G. Esposito-Farèse, Ann. Inst. Henri Poincaré Phys. Theor. **52**, 113 (1990).
  - [17] D.M. Eardley, Astrophys. J. **196**, L59 (1975).
  - [18] C.M. Will, *Theory and Experiment in Gravitational Physics* (Cambridge University Press, Cambridge, England, 1993).
  - [19] J.O. Dickey *et al.*, Science **265**, 482 (1994); J.G. Williams, X.X. Newhall, and J.O. Dickey, Phys. Rev. D **53**, 6730 (1996).
  - [20] T. Damour and N. Deruelle, Ann. Inst. Henri Poincaré **44**, 263 (1986).
  - [21] T. Damour and J.H. Taylor, Phys. Rev. D **45**, 1840 (1992).
  - [22] T. Damour and G. Schäfer, Phys. Rev. Lett. **66**, 2549 (1991).
  - [23] Z. Arzoumanian, Ph.D. thesis, Princeton University, 1995.
  - [24] N. Wex, report, gr-qc/9511017 (unpublished).
  - [25] J.H. Taylor, A. Wolszczan, T. Damour, and J.M. Weisberg, Nature (London) **355**, 132 (1992).
  - [26] J.H. Taylor, Class. Quantum Grav. **10**, S167 (1993).
  - [27] T. Damour and J.H. Taylor, Astrophys. J. **366**, 501 (1991).
  - [28] C.M. Will and H.W. Zaglauer, Astrophys. J. **346**, 366 (1989).
  - [29] T. Damour and K. Nordtvedt, Phys. Rev. Lett. **70**, 2217 (1993); Phys. Rev. D **48**, 3436 (1993).
  - [30] G.D. Coughlan *et al.*, Phys. Lett. **131B**, 59 (1983); A.S. Goncharov, A.D. Linde, and M.I. Vysotsky, *ibid.* **147B**, 279 (1984); J. Ellis, D.V. Nanopoulos, and M. Quiros, Phys. Lett. B **174**, 176 (1986); J. Ellis, N.C. Tsamis, and M. Voloshin, *ibid.* **194**, 291 (1987); T. Banks, D.B. Kaplan, and A.E. Nelson, Phys. Rev. D **49**, 779 (1994); T. Banks, M. Berkooz, and P.J. Steinhardt, *ibid.* **52**, 705 (1995); T. Banks *et al.*, *ibid.* **52**, 3548 (1995).
  - [31] L. Randall and S. Thomas, Nucl. Phys. **B449**, 229 (1995); M. Dine, L. Randall, and S. Thomas, Phys. Rev. Lett. **75**, 398

- (1995); T. Damour and A. Vilenkin, Phys. Rev. D **53**, 2981 (1996).
- [32] J.A. Frieman, C.T. Hill, A. Stebbins, and I. Waga, Phys. Rev. Lett. **75**, 2077 (1995).
- [33] S. Deser, Ann. Phys. (N.Y.) **59**, 248 (1970).
- [34] G. Esposito-Farèse, in *Proceedings of the XXVIIIth Rencontres de Moriond*, edited by J. Tran Thanh Van *et al.* (Editions Frontières, Gif-sur-Yvette, 1993), p. 525.
- [35] S. Chandrasekhar, Phys. Rev. Lett. **24**, 611 (1970); J.L. Friedman and B.F. Schutz, Astrophys. J. **222**, 881 (1978); J.L. Friedman, Commun. Math. Phys. (Germany) **62**, 247 (1978). See, however, the cautionary remarks of L. Lindblom, contribution to the Proceedings of the 14th International Conference on General Relativity, Firenze, Italy, 1995 (unpublished).